MAD/PH/374
September 1987

THE STANDARD MODEL AND PROTON-ANTIPROTON COLLIDERS IN THE ACOL/TEV I ERA

F. HALZEN, C. S. KIM

Physics Department, University of Wisconsin,

Madison, Wisconsin 53706 U.S.A.

and

J. R. CUDELL

D.A.M.T.P., University of Cambridge, Cambridge, CB3 9EW U.K.

ABSTRACT

$p\bar{p}$ collider physicists must in the near future face the question: Is there life after Tristan, SLC, LEP, and HERA? We review the main topics of $p\bar{p}$ collider physics (jets, weak bosons, and heavy quarks) concentrating on physics issues unique to hadron colliders. We emphasize the search for top. After reviewing indirect information on the top mass (from electroweak radiative corrections, ratio of $W(\to e\nu)$ and $Z(\to e^+e^-)$ events and B–$\bar{B}$ mixing) we discuss the unique opportunity to search a large fraction of the expected range 25 GeV $< m_t <$ 200 GeV in higher energy (TEV I) and higher luminosity (ACOL) experiments.

1. INTRODUCTION

Figure 1 illustrates[1] progress in measurements of parton jet cross sections since their identification in high energy $p\bar{p}$ collider events was announced by UA2 at the 1982 Paris conference. Statistics has improved and the data has explored smaller (minijets) as well as larger p_T regimes. In their first physics run, CDF has pushed[2] the measurements in Fig. 1 beyond the 10^2 GeV mark. A straightforward calculation to leading order in QCD of the inclusive parton cross section describes the measurements, provided one shops for appropriate structure functions and evolution scale in the parton flux factors ($Q^2 = p_T^2$). It is now almost fifteen years ago that Bjorken[3] dreamed up the ultimate QCD experiment in which the differential cross section $d\sigma_{ij}/d\theta$ of partons i,j in two colliding hadrons is directly measured by observing two wide-angle jets in the final state. Schematically

$$\frac{d\sigma^{\bar{p}p}}{dx_{\bar{p}}\,dx_p\,d\theta} = \sum_{ij} f_i(x_{\bar{p}}) f_j(x_p) \frac{d\sigma_{ij}}{d\theta}\,. \tag{1.1}$$

Here f_i, f_j are the probabilities for finding partons i, j in the interacting $\bar{p}$, p with momentum fractions $x_{\bar{p}}$, x_p. Even neglecting heavy quarks, the sum in Eq. (1.1) runs over 49 terms as $i, j = u, d, s, \bar{u}, \bar{d}, \bar{s}, g$ and it wass therefore considered doubtful that one can ever extract $d\sigma_{ij}/d\theta$ from experimental data. This problem is finessed by factorization,[4] indeed to a very good approximation

$$\frac{d\sigma_{ij}}{d\theta} \simeq \frac{d\sigma}{d\theta} \tag{1.2}$$

and therefore Eq. (1.1) collapses to a single term

$$\frac{d\sigma^{\bar{p}p}}{dx_{\bar{p}}\,dx_p\,d\theta} \simeq \left[\sum_i f_i(x_{\bar{p}})\right]\left[\sum_j f_j(x_p)\right]\frac{d\sigma}{d\theta}\,. \tag{1.3}$$

Equation (1.2) states that all two-body partonic cross sections (or at least those contributing significantly to Eq. (1.1)) have a universal shape. That $q\bar{q} \to q\bar{q}$, $qg \to qg$, and $gg \to gg$ have indeed to a very good approximation the same angular distribution shown in Fig. 2a. The hint in the early UA1 analysis that the agreement with Eqs. (1.2) and (1.3) is not perfect has been confirmed.[1] The origin of the clear discrepancy between theory and experiment, shown in Fig. 2b, is however not approximation (1.2); differentiating subprocesses will indeed be a heroic task, as can be judged from Fig. 1. The deviation between theory and experiment is the effect of scaling violations which are expected[4] to distort the partonic relation (1.3). This alerts us to the fact that the factorization (1.3) is a parton model result. This can be dramatically illustrated by comparing the universal 2-jet angular distribution with data[5] on $e^+e^- \to e^+e^-$ scattering. The agreement is equally satisfactory.

As a test of QCD itself, hadronic jet physics has however, reached an impasse. The reason is best illustrated by the analysis of three-jet events. Let us symbolically write Eq. (1.3) in the form

$$\frac{d\sigma^{2j}}{d(\cos\theta)} = \frac{\alpha_s^2(?)}{\hat{s}} \left[\begin{array}{c}\text{angular}\\ \text{distribution}\end{array}\right] \left[\begin{array}{c}\text{generic}\\ \text{parton distribution}\end{array}\right]. \qquad (1.3')$$

Here $\hat{s}$ is the parton c.m. energy and the angular distribution is basically the Rutherford cross section $(1-\cos\theta)^{-2}$. The three-jet $2 \to 3$ cross section σ^{3j} can be cast in the same form[6] except for the normalization which is now $\alpha_s^3(?)$. So naively the ratio $\sigma^{3j}/\sigma^{2j} = \alpha_s$; actually

$$\frac{\sigma^{3j}}{\sigma^{2j}} = \alpha_s \frac{K(3j)}{K(2j)}. \qquad (1.4)$$

The strong coupling α_s is not determined as the K factors in (1.4) are not known.

The problem is related to the choice of scale (?) in Eq. (1.3) in which α_s (and the parton distributions) run. Any choice is acceptable "?"$= p_T^2$, $\hat{s}$, $\hat{s}/4.8, \ldots$; they just represent different perturbative expansions of the all-order result which is of course independent of the choice made. This is however not the case for the leading-order calculation and in the absence of higher-order calculations the choices cannot be distinguished. The "?" can furthermore represent a different scale in the $2 \to 2$ and the $2 \to 3$ processes leading to the two unknown corrections in Eq. (1.4).

This problem has been at least partially tackled[7] for the closely related process $\bar{p}p \to \gamma X$. Prompt photon physics has a distinguished record as a test of QCD: the cross section and many other features of this process were true predictions of the theory anticipating the experiments and accommodating the results in a quantitative sense. The recent UA2 data is in agreement with the leading-order prediction[8] ($O(\alpha\alpha_s)$ diagrams in Fig. 3) made in 1978; see Fig. 4. The discrepancy between theory and experiment for $p_T \lesssim 20$ GeV was also anticipated;[9] its origin is the neglect of the $O(\alpha\alpha_s^2)$ diagrams in Fig. 3, where quarks produced with very large cross sections radiate a prompt photon. More important, however, is the fact that now Aurenche *et al.* have completed a full higher-order $\alpha\alpha_s^2$ calculation including loop diagrams.[7]

The processes $qq \to qq\gamma$ present some unique and intriguing physics opportunities.[10] The exact (not just leading log) expression for their cross section factorizes into a factor describing the interaction of the quarks and a factor containing the quark electric charges representing the radiation of the photon. For the subprocess $u\bar{d} \to u\bar{d}\gamma$ the latter factor vanishes at

$$\cos\theta_\gamma = -\frac{e_u - e_{\bar{d}}}{e_u + e_{\bar{d}}} = -\frac{1}{3}\,. \tag{1.5}$$

Here θ_γ is the angle of photon emission relative to the incident beams. Similarly the process $uu \to uu\gamma$ exhibits a "radiation" zero at $\cos\theta_\gamma = 0$. An illustrative calculation is shown in Fig. 5. This process is the hadron collider's answer to $\gamma\gamma$ physics at e^+e^- machines. The squared matrix element has indeed two electric couplings as shown in Fig. 6, leading not only to contributions proportional to $Q_i^2\alpha$, $Q_j^2\alpha$, but also to $Q_iQ_j\alpha$.

The vanishing cross section (1.5) is a result of the Q_iQ_j term cancelling Q^2 terms. This charge correlation $\langle Q_iQ_j\rangle$ depends on the electric charge of colored quarks and not just on the color averaged charge as in the R-measurement in $e^+e^- \to$ hadrons.

The excursion by the UA1 experiment into the small p_T regime of jet physics, see Fig. 1, sparked a resurgence of interest in minimum bias physics. The "mini-jet" problem predates[11] QCD as we know it today and is illustrated in Fig. 7 with two illustrative calculations. In Fig. 7a we calculate the inclusive two-jet cross section in $p\bar{p}$ collisions. The jets are required to have a minimum transverse momentum $p_{T\,\mathrm{min}}$ and

$$\sigma_{\mathrm{jet}}\,(p_T > p_{\mathrm{min}}) = \int\limits_{p_{T\,\mathrm{min}}} \frac{d\sigma^{\mathrm{QCD}}}{dp_T}\,dp_T\,. \tag{1.6}$$

σ^{QCD} represents the standard leading order two-jet cross section calculated in perturbative QCD. While cross sections are familiarly small at ISR energies, they rise above 10 mb for $p_{T\,\mathrm{min}} \simeq 3$ GeV at $\sqrt{s} = 540$ GeV and become similar in magnitude to $\sigma_{\mathrm{inel}} \simeq 40$ mb; see Fig. 7a. Alternatively, even for $p_{T\,\mathrm{min}} >$

10 GeV the jet yield exceeds 10 mb for $\sqrt{s} = 40$ TeV, as can be concluded from Fig. 7b. At SSC energy $\sqrt{s} = 40$ TeV the inclusive jet cross section is 100 mb for $p_{T\,\mathrm{min}} \simeq 6$ GeV. This is a cross section of order σ_{tot}.

These observations open a new frontier of jet physics. On the theoretical side one must question whether the estimates in Fig. 7 are theoretically sound for $p_{T\,\mathrm{min}} \ll \sqrt{s}/2$. After all, σ_{jet}, as defined by (1.6), diverges for $p_{T\,\mathrm{min}} \to 0$. There is no *a priori* problem with large inclusive cross sections—there is no such thing as a Froissart bound for an inclusive cross section. It could exceed σ_{tot} or it has even been speculated[11] that jets are the origin of the rise of σ_{tot} with energy; see Fig. 8. This is an unresolved problem.[12] The proliferation of soft gluons is the origin of the large cross sections in Fig. 7. It has been shown[13] that this is calculable all the way down to p_T values satisfying

$$\Lambda_{\mathrm{QCD}} \lesssim p_T\,. \tag{1.7}$$

Large inclusive jet cross sections for small $x = 2p_T/\sqrt{s}$ are a prediction of QCD and not just the consequence of an excursion of the calculations in a dangerous kinematic regime. Minimum bias events are expected to be rich in structure at future colliders like SSC or LHC, thus interfering with physics triggers either directly or via overlapping events in a single beam crossing.

2. INTERMEZZO

The remaining topics in this review have a common theme: the top quark. The first run of Tristan[14] increased the experimental lower limit on the mass of the top

$$25 \text{ GeV} < m_t \,. \tag{2.1}$$

The top and the elusive Higgs form the last missing pieces in the almost complete complete standard model puzzle. As the Higgs could have a mass in the TeV-range its discovery might have to await commissioning of a new generation of supercolliders. In contrast there is a feeling in the air that the top quark is within our grasp with Tristan boosting its energy to 33 GeV and with SLC, LEP, and higher energy/luminosity $p\bar{p}$ colliders in our near future. It is therefore timely to review the indirect information we have on the mass of the top. The following conclusions are relatively easy to reach and basically uncontroversial:

i) study of the radiative corrections to the standard electroweak model implies that m_t cannot exceed a mass of a few hundred GeV, with updated experimental input

$$m_t < 200 \text{ GeV} \,; \tag{2.2}$$

ii) data on the ratio of $W(\to e\nu)$ and $Z(\to e^+e^-)$ events produced in $p\bar{p}$ collisions favor a low top mass. Typically $m_t < m_W$ with preference for the lowest values consistent with (2.1);

iii) the observation of B–$\bar{B}$ mixing, with $B \equiv B_d(b\bar{d})$, combined with theoretical prejudice regarding the structure of the KM matrix and the values

of the parameter $f_B^2 B_B$ describing the binding of $b\bar{d}$ quarks in B-mesons, casts doubt on whether the top can be lighter than 50 GeV or so;

iv) UA1 data actually exclude a top in this mass range provided its production cross section is "within a factor" of the calculated value (meaning the Eurojet Monte Carlo value).

This is the easy part; more difficult is to assess how compelling limits *i*)-*iv*) are. This is the main goal of this review. The issue is critical as a non-critical interpretation of *i*)-*iv*) readily leads to the conclusion that 50 GeV $\lesssim m_t \lesssim M_W$ putting Tristan, SLC, and LEP out of business as far as a top search is concerned. The discussion will then naturally cover the following topics:

- A limit like (2.2) from electroweak radiative corrections is difficult to avoid. In an even more positive vein we look into the future at ACOL[15] and CDF experiments accumulating 10^4 W's and 10^3 Z's in $p\bar{p}$ collisions. They could determine the top mass from radiative corrections via a precision measurement of M_W/M_Z combined with a value of M_Z known to 50 MeV from SLC or LEP.
- The ratio of W-to-Z events of "number of neutrinos fame" favors a low value of m_t. The statistical significance of this statement depends however on the value of the production ratio σ_W/σ_Z calculated in the framework of perturbative QCD. Although this ratio is insensitive to u-, d-quark structure functions, it crucially depends on the difference between u and d. First observed in the historic SLAC-MIT measurement of F_2^n/F_2^p, this difference has been determined by at least seven deep inelastic scattering experiments in the last 15 years. We use this data to reevaluate σ_W/σ_Z and assess the significance of limits on the number of neutrinos as well as the mass of the

top.

- A discussion of the significance of the $m_t \gtrsim 50$ GeV limit from B-$\bar{B}$ mixing is straightforward. The limit is extracted from the measurement of $\frac{\Delta M}{\Gamma}$ via a computation of the $\Delta B = 2$ box diagram. This relation involves quantities with experimental errors, *e.g.* the KM matrix elements. Even ignoring theoretical ambiguities we show how mass values of 25 or 30 GeV are ruled out to no better than 2σ even if your pocket calculator tells you that $m_t \gtrsim 55$ GeV.
- We finally review the present status of calculating heavy quark production cross sections in perturbative QCD. The question is central as the non-observation of top in the UA1 experiment can only be translated into a lower limit on m_t via a calculated value of the cross section.

In the end it is difficult to draw any definite conclusions except maybe that no experimenter should feel discouraged searching any mass range between 25 and 200 GeV. This is good news for the e^+e^- experiments but also for hadron colliders. With increased energy (Fermilab) and luminosity (CERN) they can cover more than half of this range. We discuss this in some detail.

3. ELECTROWEAK RADIATIVE CORRECTIONS

In the standard electroweak model a precision measurement of the mass values M_W and M_Z can also fix the top mass. The most direct way to achieve this is to compute the muon lifetime $\mu \to e\bar{\nu}_e\nu_\mu$ to one loop order; see Fig. 9. To this order the calculated lifetime receives contribution from $t\bar{b}$ loops inserted into the leading W-exchange diagram and from diagrams containing the Higgs boson ϕ. This is sketched in Fig. 9. For the problem under consideration it

is nice to proceed with the calculation just like in QED and to choose the fine structure constant α and the masses entering the problem (M_W, M_Z, m_ϕ, and the fermion masses including m_t) as the renormalization parameters to be fixed by experiment. The explicit expression is complicated[16] but of the form

$$\Gamma_{th}(\mu \to e\nu\bar{\nu}) = \Gamma(\alpha,\ M_W,\ M_Z,\ m_t,\ \eta\!\!\!/_\phi)\ . \tag{3.1}$$

Here we have suppressed the dependence on known quark and lepton masses. As all the external particles are light it is not too surprising that (3.1) depends very weakly on the Higgs mass; its role can be safely ignored. By identifying Γ_{th} with the experimental value of the muon lifetime

$$\Gamma_{th}(\mu \to e\nu\bar{\nu}) = \Gamma(\text{exp})\ , \tag{3.2}$$

we obtain a mass formula relating M_W, M_Z, and m_t. This is shown in Fig. 10. Given a value of M_Z, which will be determined by SLC/LEP to 50 MeV precision, a relation between M_W and m_t is obtained. This relation is to be compared with the tree level prediction, *i.e.* the first diagram in Fig. 9, which is of course independent of m_t. When m_t becomes very large, perturbation theory breaks down resulting in very large unphysical mass values M_W; see Fig. 10. Because of uncertainties in the energy scale, experiments determine the ratio M_W/M_Z with better precision. We therefore replot in Fig. 11 the mass formula of Fig. 10 as a relation between M_W/M_Z and m_t for $M_Z = 91.5 \pm 1.2$ GeV, the present UA2 value.[18] The value of M_W/M_Z is consistent within 1σ with their measured value (shown as the horizontal band in Fig. 11) provided $m_t \lesssim 300$ GeV. Larger values of m_t are already excluded by the UA2 measurements. Using information

from neutrino experiments this bound can be reduced[19] to 200 GeV as previously quoted in (2.2).

By looking at Fig. 11 one can visualize what happens when in the near future the experimental errors on M_W/M_Z and M_Z are reduced. The band of M_W/M_Z values will shrink and so will the error on the relation between M_W/M_Z and m_t which reflects the error on M_Z. *E.g.*, if the UA2 errors shrink to the present values we would conclude that $m_t \simeq 40$ GeV, *i.e.* the m_t value where $\frac{M_W}{M_Z} = \frac{80.2}{91.5}$ for $M_Z = 91.5$ GeV. If this is indeed the value of the observed top mass we have measured the radiative corrections and hence tested the gauge structure of the electroweak model. This is at present not possible.[20]

This gedanken experiment with the UA2 errors will hopefully be performed in the ACOL experiments. On the basis of a simulation of $10^4 W$ and $10^3 Z$ events in the upgraded UA2 detector a precision of

$$\Delta\left(\frac{M_W}{M_Z}\right) = 1.5 \times 10^{-3} \tag{3.3}$$

has been projected.[21] This statistic corresponds to the 20 pb^{-1} integrated luminosity expected with the ACOL $\bar{p}$-accumulator. We can therefore look forward to a determination of the weak boson masses to precision $\Delta(M_Z) \simeq 50$ MeV by SLC and LEP and $\Delta M_W \simeq 150$ MeV from (3.3). More conservative estimates foresee $\Delta M_W \simeq 350$ MeV. These errors are not much wider than the draftsman's pen in Fig. 11. The UA2 gedanken experiment will soon be reality and this approach could reveal the top mass, possibly prior to its discovery.

4. NEUTRINO LIMITS AS A HANDLE ON THE TOP MASS

The discovery of the W, Z delivered an unexpected bonus: more precise information on the number of light neutrinos. It is shocking to imagine that pre-1983 our best limit from a terrestrial experiment was that $N_\nu < 1400$, a result obtained from failure to detect[22] the decay $K \to \pi\nu\bar{\nu}$. Of course standard cosmology and measurements of the abundance of light elements such as He imply $N\nu < 4$ or even $N_\nu < 3$ according to some analyses. (This would imply that $\nu_\tau = \nu_\mu$ (or ν_e).) SN 1987 told us in about 3 seconds that $N_\nu < 10$. The total binding energy of a neutron star would be insufficient to yield the observed $\bar{\nu}_e$ pulse if ν_e, $\bar{\nu}_e$ had to share their energy with more than about 10 other neutrino species. Present e^+e^- collider experiments claim[23] $N_\nu < 5$. Although it is not easy to improve on this by counting W and Z events in $p\bar{p}$ collisions, we here want to emphasize the relevance of this procedure to the top mass.

The whole game is based on an identity

$$R \equiv \frac{\#W \to e\nu}{\#Z \to e^+e^-} = \frac{[\Gamma(W \to e\nu)/\Gamma(W)]}{[\Gamma(Z \to e^+e^-)/\Gamma(Z)]}\frac{\sigma_W}{\sigma_Z}\,. \tag{4.1}$$

The experimentalist measures R by counting W and Z events in $p\bar{p}$ interactions. The right-hand-side is a standard model prediction. The ratio of branching ratios is determined by the standard electroweak couplings and the ratio of cross sections is computed in perturbative QCD. So (4.1) represents a powerful test of the standard model except for 3 ambiguities:

i) we do not know if $N_\nu = (2)$, 3, or 4, which affects the value of Γ_Z;

ii) we do not know the top mass and therefore the contribution of the decays $W \to t\bar{b}$ and $Z \to t\bar{t}$ to Γ_W and Γ_Z is not fixed;

iii) QCD predicts $\sigma(q\bar{q} \to W)/\sigma(q\bar{q} \to Z)$ not $\sigma(p\bar{p} \to W)/\sigma(p\bar{p} \to Z)$ which enters in (4.1). We tackle this last point first.

The ratio of W to Z cross sections must be one of the most reliable predictions of QCD as every diagram producing a W also produces a Z up to $O(\alpha_s^2)$ where the additional diagrams shown in Fig. 12 produce Z via a quark loop. Therefore,

$$\frac{\sigma(q\bar{q} \to W)}{\sigma(q\bar{q} \to Z)} = \begin{bmatrix}\text{ratio of known} \\ \text{couplings}\end{bmatrix} + O(\alpha_s^2)\left[\frac{m_t^2 - m_b^2}{m_Z^2}\right] . \tag{4.2}$$

The cross sections are the same up to known standard model couplings. Even the diagrams in Fig. 12 contributing to the difference to $O(\alpha_s^2)$ would vanish as a result of the anomaly cancellations of the fermions in the triangle. Only the (t, b) generation contributes because of the t, b mass difference; see (4.2). The real ambiguity resides in the parton flux factors relating $q\bar{q}$ and $p\bar{p}$ cross sections. This flux factor is of the form $(u\bar{d} + \bar{u}d)/(u\bar{u} + d\bar{d})$ and therefore depends on the ratio u/d rather than on u and d individually. It is well known that this ratio can be extracted from data on F_2^p and F_2^n measured in leptoproduction experiments. The ratio u/d can also be calculated from simultaneous measurements of ν and $\bar{\nu}$ interactions on H and D targets. We used[24] these experiments individually to calculate σ_W/σ_Z; the results are shown in Fig. 13. We assumed that $M_W = 80.1$ GeV and fixed M_Z from the value of $\sin^2\theta_W = 0.232$. The errors on the individual points in Fig. 13 reflect not only the errors on the leptoproduction data but also any ambiguities intrinsic to the extraction of u/d, *i.e.* the parametrization of u, d individually, the separation of valence and sea-quarks and the interpolation of the data in x. For a detailed discussion see Ref. 25. The average of all points yields $\sigma_W/\sigma_Z = 3.42 \pm 0.01$. This ignores the errors on σ_W/σ_Z connected with $M_W\,(\pm 0.02)$ and $\sin^2\theta_W$ (± 0.04) so that our final result

can be stated as follows:

$$\frac{\sigma_W}{\sigma_Z} = 3.42 \pm 0.05 + \epsilon\,. \tag{4.3}$$

Here ϵ represents a small contribution from W, Z production via $c\bar{s}$ and $c\bar{c}$, respectively. It cannot be reliably calculated, is positive and smaller than the error in (4.3).[26] This result agrees with similar analyses in Refs. 25 and 27 where

$$\frac{\sigma_W}{\sigma_Z} = 3.41 \pm 0.08\,. \tag{4.4}$$

Individual experiments in Fig. 13 have systematic errors of a few percent. One can hope that they have been averaged. Adding them does not change the results significantly as the error in (4.3) is dominated by errors on M_W, M_Z. Conservatively we will use (4.4) for further discussion.

We are now ready to compute the right-hand-side of (4.1). Figure 14 exhibits R as a function of m_t assuming that $N_\nu = 3$. The rise in R above $m_t \simeq \frac{M_Z}{2}$ is a result of switching of the decay $Z \to t\bar{t}$ while $W \to t\bar{b}$ is still kinematically allowed. When for $m_t > M_W - m_b$ both decays are forbidden, R becomes independent of m_t. The 1σ error on the calculation is a combination of the error on σ_W/σ_Z in (4.3) and errors on the ratio of branching ratios from $\sin^2\theta_W$ and $\Lambda_{\rm QCD}$. The latter enters via a factor $(1 + \alpha_s/\pi)$ when taking into account the higher order correction to W, $Z \to q\bar{q}'$ decay rates. The right-hand-side of (4.1) is measured to be

$$R(\text{exp}) = 8.4^{+1.1}_{-0.9} \tag{4.5}$$

from the combined CERN collider experiments.[28] It is beyond controversy that the low value of R (exp) favors low values of m_t. The more difficult question is to

assess the statistical significance of this statement. An obvious thing to do is to calculate the overlap of R (calc) and R (exp) assuming they are Gaussian of width 1σ. The result is shown in Fig. 15. Values of $m_t > m_W$ have a probability of less than 5%. In this exercise 100% corresponds to R (calc) = R (exp) with equal errors. As the e^+e^- experiments are still consistent with $N_\nu = 4$ we repeated the exercise for this assumption. Clearly the case for a light top is now strengthened as an additional neutrino increases R beyond the already large values obtained in Fig. 14 assuming $N_\nu = 3$.

The only firm conclusion is that low experimental values of R favor a light top.[29] It is puzzling that the most probable values in Fig. 15 are for m_t-values already excluded by Tristan. Are we fooled by low statistics (*e.g.* the low number of Z-events) or by naive manipulation of error bars (*e.g.* leading to (4.3) or (4.4))? Is $N_\nu = 2$ or is there some new physics affecting the ratio of branching ratios in (4.1)? We are looking towards a future where the top mass is known and (4.1) can actually be used to hunt for new physics. This new physics is not necessarily present in observable decays of W or Z. The Z couplings in (4.1) could be reduced by mixing with a heavier Z'. This could reduce R (calc) and not lead to observable physics below M_Z. A sample calculation[30] is shown in Fig. 16 where the Z mixes with Z' related to a U(1) in the $E(6)$ decomposition chain $E(6) \to \mathrm{SO}(10) \to \mathrm{SU}(5) \times \mathrm{U}(1)$. Notice that $m_t < M_W$ is still favored!

The fact that many ambiguities (*e.g.* K factors) cancel in the ratio of W, Z cross sections can also be exploited to test the standard model and count neutrinos using their production with large p_T. For $\sqrt{s} = 540$ GeV the large p_T cross sections are calculable from leading-order perturbation theory for $p_T \gtrsim 25$ GeV. *I.e.* here multigluon emission does not significantly modify the result computed

from the leading-order $q\bar{q} \to (W, Z) + g$ and $qg \to (W, Z) + q$ diagrams. The effect would cancel in the W-to-Z ratio anyway. The cross sections are shown in Fig. 17 in the form of the number $W \to e\nu$ and $Z \to \nu\bar{\nu}$ monojet events as a function of p_T for $\sqrt{s} = 630$ GeV. The $W \to e\nu$ large p_T cross section agrees well with the observations[31] of both UA1 and UA2. More interesting, however, is that the equality of the large p_T yields

$$B(W \to e\nu)\frac{d\sigma}{dp_T}(W^\pm) = B(Z \to \nu\bar{\nu})\frac{d\sigma}{dp_T}(Z)\,, \tag{4.6}$$

shown in Fig. 17. What is the origin of this equality?[32] In the limit $M_W \simeq M_Z$ and $u(x) \simeq d(x)$ we derive

$$\frac{B(Z \to \nu\bar{\nu})d\sigma(Z)/dp_T}{B(W \to e\nu)d\sigma(W)/dp_T} = \frac{3}{4(1-x_W)}\frac{1}{\cos^2\theta_c}\left[1 + O(x_W^2)\right]. \tag{4.7}$$

Here $x_W = \sin^2\theta_W$ and (4.6) follows from the fact that $x_W \simeq \frac{1}{4}$ and the Cabibbo angle $\cos^2\theta_c \simeq 1$. Corrections for $M_W \neq M_Z$ and $u(x) \neq d(x)$ have opposite signs and cancel approximately. Again relation (4.6) depends on $N_\nu = 3$. Tests of (4.6) involve measurement of the monojet cross section $Z(\to \nu\bar{\nu})$ + gluon by the missing p_T technique. A large background from $W \to \tau\nu_\tau$ events has to be subtracted. Nevertheless, experiments are reaching the sensitivity to test (4.6). In the meantime, it provides us with a way to estimate the standard model monojet rate and count neutrinos with ACOL statistics to better than $\Delta N_\nu < 1$.

5. B-$\bar{B}$ MIXING AND THE CASE AGAINST A LIGHT TOP

The case for a light top, just presented, challenges a bandwagon of papers[33] arguing for large values of m_t on the basis of the recent observation of B-$\bar{B}$ mixing.[34] Here $B = B(b\bar{d})$. As large means 50 GeV or even less, there is no real conflict. There is even less of a confrontation after realizing that 50 GeV can mean 30 GeV at a 2σ level as we will show below.

There is no doubt that the procedure of extracting information on heavy quark masses from $\Delta S = 2$ weak matrix elements has a proven and most distinguished record. In Fig. 18 we are reminded that the box diagram involving a charm quark contributes to K-$\bar{K}$ mixing and it was realized prior to its discovery that this contribution, proportional to m_c^2, would result into a too large mass difference ΔM unless the c-quark was relatively light. Through the CP-violation parameter ϵ the K-$\bar{K}$ system also yields information on top. Similar arguments are now used to close in on the value of m_t from the box-diagram dominating a calculation of B-$\bar{B}$ mixing; see Fig. 18. The result of ARGUS[34] that

$$\frac{\Delta M(B-\bar{B})}{\Gamma} = 0.73 \pm 0.18 \tag{5.1}$$

must be accommodated by the box-diagram in Fig. 18; in a somewhat simplified form[35]

$$\frac{\Delta M}{\Gamma} = \left[\frac{G_F^2 m_B \tau_B}{6\pi^2}\right] \left[f_B^2 B_B\right] |V_{tb}^* V_{td}|^2 \, m_t^2 \, . \tag{5.2}$$

This assumes of course that no new physics involving new interaction (charged Higgs) or new particles in the box (fourth generation, superparticles, ...) is actually the origin of (5.1). The proportionality constant relating $\Delta M/\Gamma$ and

m_t^2 contains several factors. The first factor contains known quantities including the B-lifetime τ_B. The second factor describes the binding of $b\bar{d}$ quarks inside B-mesons, this factor cannot be computed in any straightforward manner. One guesses that $f_B \gtrsim f_\pi \simeq m_\pi$ and that B is $O(1)$. The third factor contains the KM matrix elements relating t to b and d. As the top has not been observed they must be inferred from the unitarity of the KM matrix. To illustrate how m_t is restricted by (5.2) we can assume the Wolfenstein form of the KM matrix with $V_{tb} = 1$ and $V_{td} = V_{bu}$ as the matrix is symmetric. As we know that $0.07 < V_{bu}/V_{bc} < 0.2$ from experiment[34] (where V_{bc} is fixed by the b-lifetime), we can now evaluate the factor relating $\Delta M/\Gamma$ to m_t^2 and conclude that $m_t \geq 55$ GeV for the measured value (5.1). This is easy. The obvious question is, however, to ask what remains of this result when one includes experimental errors on all input quantities and does not introduce unproven assumptions such as $V_{td} = V_{bu}$. This requires using unitarity of the KM matrix only and reconsidering the determination of its matrix elements ab initio.

The problem is straightforward[36] and charted in Tables 1a and 1b. The input quantities in (5.2) including those required to determine the KM matrix elements fixing V_{tb}, V_{td} by unitarity, are listed with errors in Table 1a. We included the CP-violation parameter ϵ along with $\Delta M/\Gamma(B$-$\bar{B})$ to constrain the value of m_t. This data is subsequently fitted to all parameters in the problem (listed in Table 1b) for different values of m_t. One soon realizes that including all errors (Table 1a) and varying all parameters simultaneously (Table 1b) introduces considerable freedom in the problem. No statistically significant bound can be obtained exceeding 25 GeV. Sample calculations are shown in Fig. 19. Assuming standard prejudice like $f_B^2 B < 0.04$ and $B_K < 1$ we conclude that

$$m_t > 30 \text{ GeV at } 1\sigma \text{ level},$$
$$m_t > 24 \text{ GeV at } 2\sigma \text{ level}. \tag{5.3}$$

Using a pocket calculator and ignoring statistics one would naively conclude that $m_t \gtrsim 50$ GeV. For $f_B^2 B < 0.06$ values down to the Tristan limit of 25 GeV are allowed at the 1σ level. We still exclude 30 GeV only at the 2σ level when pushing $f_B^2 B$ down to a value of 0.03. The conclusion is straightforward. Discovery of the top will provide constraints on the parameters f_B^2, B in (5.1) which are unfortunately not calculable in perturbation theory. Although masses below 30 GeV seem to be disfavored, see Fig. 19, the statement is statistically weak especially as our statistics ignore theoretical ambiguities related to approximations made in computing ϵ, QCD-corrections, ...

The messages on the top mass from W, Z production and B-$\bar{B}$ mixing are conflicting. Neither seem compelling so at present (2.1) and (2.2) still define the useful range of masses for top hunting. In that range UA1 has made an extensive and unsuccessful search.[37] We discuss this next.

6. $p\bar{p}$ COLLIDER SEARCHES FOR TOP: PRESENT AND FUTURE

The standard signature for top searching in hadron collisions is one (or two) prompt leptons from the semi-leptonic decay of one (or both) associatively produced heavy quarks, *i.e.*

$$p\bar{p} \to Q\bar{Q}X \quad \begin{matrix} \nearrow \bar{\mu}\nu Q' \\ \searrow \mu\bar{\nu}\bar{Q}' \end{matrix} . \tag{6.1}$$

Here $Q = c$, b, or t. There is a theorem[38] that in QCD a heavy quark is the

heavier quark's fatal background. A high p_T lepton from t cannot be distinguished from a leptonic decay of a high p_T c- or b-quark. Therefore a prompt lepton search inevitably includes further study of the associated hadrons in the event. Strategies have been pioneered and refined by the UA1 experiment and resulted in a negative search.[37] A negative search can be translated into a mass limit provided one has a theoretical calculation of the expected yield of t-quarks decaying in the detector. This is illustrated in Fig. 20 where the observed prompt muon and dimuon cross section are compared with the expected[39] yield from c, b decays. c, b production is calculated to $O(\alpha_s^3)$ from the diagrams in Fig. 21a. A possible additional prompt lepton contribution from a top quark in the 23-40 GeV mass range is shown as the dashed area in Fig. 20. Although the fit to single μ's seems to be improved by adding top, an excess of dimuon events over the rate observed excludes this possibility. This conclusion is reinforced[37] by a study of the associated hadrons in the events, *i.e.* by imposing isolation cuts on the hadrons routinely accompanying high momentum c, b quarks faking top.

Although we have no criticism of this analysis we would like to make two observations. As a study of rates alone is inconclusive, see Fig. 20, requiring the absence of hadronic activity in the direction of the lepton expected in c, b decays is crucial. While this might be possible for a heavy top, it is a difficult procedure for a 25 GeV quark. Not only is one dealing with accompanying jet activity which is relatively weak, but the problem of fake isolation resulting from mismeasurement of the accompanying jet axis becomes more severe for the softer jets associated with the background to a top as light as 25 GeV. The limits must be weaker at 25 GeV than at 45 GeV. Is there a low mass window? Secondly, any limit depends on the calculated cross section as illustrated in Fig. 20. The top

is excluded by the dimuon sample because of the large cross section associated with higher order $O(\alpha_s^3)$ $2 \to 3$ processes. How credible are the calculations? We review this briefly.

There is no doubt that any realistic calculation of heavy quarks has to include $O(\alpha_s^3)$ as well as the "leading order" $O(\alpha_s^2)$ fusion diagrams in Fig. 21a. The $O(\alpha_s^3)$ diagram shown can be visualized as a two jet event where a final state gluon jet has a $Q\bar{Q}$ pair among its fragmentation products. For charm this occurs for only 10% of the jets but the underlying two jet cross section is large compared to gluon fusion. The problem has been demonstrated[40] with a sample of events with a heavy quark Q produced opposite a jet with $p_T \geq p_{T\min}$. As shown in Fig. 21b the opposite jet is a gluon (or quark) jet when Q is produced via the $2 \to 3$ process and is the associated quark for production via gluon fusion. The $2 \to 3$ process dominates[40] in data samples with $p_{T\,\min} = 7$ GeV. There is really no surprise here, the $O(\alpha_s^2)$ and $O(\alpha_s^3)$ graphs represent different production mechanisms and there is no implication for the convergence of perturbation theory. The result should be familiar from QED. When high energy γ's interact with matter $O(\alpha^3)$ pair production $\gamma Z \to e^+e^-Z$ dominates the $O(\alpha^2)$ Compton process $\gamma e \to e\gamma$; see Fig. 22. The dominance of the $(2 \to 3)$ process in QCD is reinforced by a relative color factor between the $gg \to gg$ two-jet and the $gg \to Q\bar{Q}$ fusion processes, which happens to be 104:

$$\frac{\sigma(gg \to gg)}{\sigma(gg \to Q\bar{Q})} = \frac{27N^3}{N^2-2} = 104\,. \tag{6.2}$$

The previous discussion alerts us to the necessity of calculating heavy quark cross sections to $O(\alpha_s^3)$. In calculating the total cross section $p_{T\,\min} \to 0$ and the $2 \to 3$ process diverges as the gluon accompanying the $Q\bar{Q}$ pair becomes soft.

In the Eurojet calculation[39] used by UA1 and shown in Fig. 20 $p_{T\,\min}$ has been treated as a parameter and fixed at 3 GeV for no compelling reason. Although this is at present the best one can do, this procedure doesn't even correctly address the problem of how to "add" $(2 \to 2)$ and $(2 \to 3)$ processes. As this is a field theoretic calculation the $(2 \to 3)$ process can subtract from the leading order result.

The issue is obviously important for any conclusions drawn from Fig. 20. The theoretical problem is illustrated in Fig. 23 where the $O(\alpha_s^3)$ $gg \to Q\bar{Q}g$ has been redrawn in a suggestive way. When the virtual exchange gluon is close to its mass shell, *i.e.* almost a real gluon, then the circled vertex in Fig. 23 becomes part of the gluon structure function and the diagram has already been included via the evolved structure function in the leading $gg \to Q\bar{Q}$ diagram. In theorist language one has to remove the mass singularities from the $2 \to 3$ graphs. The left-over part, which can have either sign, should be added to the $O(\alpha_s^2)$ diagrams. This as well as a calculation of the virtual diagrams has not been done. A partial calculation of the $gq \to Q\bar{Q}q$ subset of diagrams has been completed.[41] This $O(\alpha_s^3)$ contribution actually subtracts from the leading order result. The complete answer is unknown and can certainly not be mimicked by a p_T-cut. Mass limits involving a calculation of the cross section should be treated with care and regarded as preliminary.

There is however some good news for $p\bar{p}$-experiments in all this. Whereas SLC, LEP can explore masses to about $M_Z/2$ (Tristan will reach 33 GeV by Fall 1988), $p\bar{p}$ colliders can reach masses all the way to M_W and even higher by searching for decays $t \to Wb$. Despite all the warnings about cross section calculations we use leading order calculations as a guide and predict[42] $10^3 \sim 10^4$

tops (mass 40 GeV) in CDF (because its increased energy) and in UA1/2 (because of the expected increase in luminosity from 750 nb^{-1} to 20 pb^{-1}); see Fig. 24. This increase opens up searches involving dileptons with meaningful statistics. With a 10% average leptonic branching ratio we can expect $10 \sim 10^2$ $\mu^+\mu^-$, e^+e^-, and more important $e\mu$ events. Some sample predictions[43] are shown in Fig. 25. If the chance of discovery is proportional to the fraction of mass range 25-200 GeV, hadron colliders are still our best shot at the top.

ACKNOWLEDGEMENTS

This research was supported in part by the University of Wisconsin Research Committee with funds granted by the Wisconsin Alumni Research Foundation, and in part by the U. S. Department of Energy under contract DE-AC02-76ER00881.

REFERENCES

1. W. Scott, Les Rencontres de Physique de la Vallée d'Aoste, La Thuile, Italy (1987).
2. S. H. Kim, *Physics in Collision*, Tsukuba, Japan (1987).
3. J. D. Bjorken, Phys. Rev. **D8**, 4098 (1973).
4. F. Halzen and P. Hoyer, Phys. Lett. **B130**, 326 (1983); B. Combridge and C. Maxwell, Nucl. Phys. **B239**, 429 (1984).
5. M. Delfino, University of Wisconsin (thesis).
6. B. Combridge and C. Maxwell, Nucl. Phys. **B151**, 299 (1985).
7. P. Aurenche *et al.*, Phys. Lett. **B140**, 87 (1984).
8. F. Halzen and D. M. Scott, Phys. Lett. **B78**, 318 (1978).
9. A. P. Contogouris *et al.*, Phys. Rev. **D25**, 990 (1982); M. Dechantsreiter *et al.*, Phys. Rev. **D24**, 2856 (1981); R. Gandhi *et al.*, Phys. Lett. **B152**, 261 (1985).
10. K. Hagiwara *et al.*, Phys. Lett. **B135**, 324 (1984).
11. D. Cline, F. Halzen, and J. Luthe, Phys. Rev. Lett. **31**, 491 (1973).
12. For recent reviews, see A. Mueller, in *Lepton-Photon Symposium*, Kyoto, edited by M. Konuma and K. Takahashi, World Scientific, Singapore (1985); A. Mueller in *Proceedings of the DPF Meeting*, Eugene, Oregon (1985); J. C. Collins, Supercollider Physics, edited by D. Soper, World Scientific, Singapore (1986) and UCLA SSC Workshop, Los Angeles (1986); F. Halzen, and C. S. Kim, *Les Rencontres de Physique de la Vallée d'Aoste*, La Thuile, Italy (1987).

13. L. V. Gribov, E. M. Levin, and M. G. Ryskin, Phys. Rep. **100**, 1 (1983).

14. K. Amako, A. Miyamoto, and Y. Sakai, "Physics in Collision," Tsukuba, Japan (1987).

15. ACOL is the new $\bar{p}$-accumulator at CERN.

16. K.-I. Aoki *et al.*, Prog. Theor. Phys. Suppl. No. **73** (1982).

17. F. Halzen, Z. Hioki, and M. Konuma, Phys. Lett. **126B**, 129 (1983).

18. UA2 collaboration: prersented by S. Loucatos at 6th $p\bar{p}$ Workshop, Achen (June 1986).

19. P. Langacker, W. M. Marciano, and A. Sirlin, University of Pennsylvania preprint UPR-0334T (1987).

20. In future collider runs the associated production $u\bar{d} \to W\gamma$ and the W-decay $W \to u\bar{d}\gamma$ provide alternate possibilities to probe the gauge structure of the electroweak model. A radiation zero in the photon angular distribution, similar to the one discussed in §1, provides the experimental signature. See *e.g.* J. Cortez, K. Hagiwara, and F. Herzog, Nucl. Phys. **B278**, 26 (1986).

21. P. Jenni, CERN-EP/87-29 (1987).

22. Y. Asano *et al.*, Phys. Lett. **107B**, 159 (1981).

23. T. Lavine, University of Wisconsin (thesis); CELLO collaboration: contributed to the 1987 Lepton and Photon Symposium, Hamburg (1987).

24. We follow the method described in Ref. 25 which also contains references to the data.

25. F. Halzen, C. S. Kim, and S. Willenbrock, Phys. Rev. **D37**, xxx (January 1988)

26. For further analysis we take $\epsilon = 0$. It is easy to verify that $\epsilon > 0$ will strengthen limits on N_ν and m_t.

27. A. D. Martin, R. G. Roberts, and W. J. Stirling, Durham preprint DTP/87/18 (1987).

28. See Ref. 18 and UA1 collaboration: presented by D. Denegri at 6th $p\bar{p}$ Workshop, Achen (June 1986).

29. F. Halzen, Phys. Lett. **182B**, 388 (1986).

30. M. Drees and X. Tata, private communication.

31. UA2, M. Mohammadi, University of Wisconsin (thesis); H. Plothow-Besch, 5th Topical Workshop on $p\bar{p}$ Collider Physics, Saint-Vincent, Aosta Valley, 1985, M. Greco, Editor, World Scientific, Singapore.

32. F. Halzen and K. Hikasa, Phys. Lett. **B168**, 135 (1986).

33. For a review see J. Ellis, J. B. Hageline, and S. Rudaz, Phys. Lett. **B192**, 201 (1987); I. I. Bigi and A. I. Sanda, Nucl. Phys. **B281**, 41 (1987); D. Du and Z. Zhao, Phys. Rev. Lett. **59**, 1072 (1987); J. Maalampi and M. Roos, Phys. Lett. **B195**, 489 (1987); V. Barger, T. Han, D. V. Nanopoulos, and R. J. N. Phillips, Phys. Lett. **B194**, 312 (1987); L. L. Chau and W.-Y. Keung, UC-Davis preprint UCD-87-02; G. Altarelli and P. J. Franzini, CERN-TH.4745/87; K. Hagiwara, KEK-TH-170.

34. H. Kapitza, "Physics in Collision," Tsukuba, Japan (1987); ARGUS collaboration, H. Albrecht *et al.*, DESY-87-029, Phys. Lett. **B192**, 245 (1987).

35. Explicit calculations include non-leading terms as well as QCD corrections.

36. J. R. Cudell *et al.*, Madison preprint MAD/PH/352, Phys. Lett. B (to be published).

37. K. Eggert, "Physics in Collision," Tsukuba, Japan (1987).

38. S. Pakvasa *et al.*, Phys. Rev. D **20**, 2862 (1979).

39. B. Van Eyck, University of Amsterdam, thesis (1987).

40. F. Halzen and P. Hoyer, Phys. Lett. **154B**, 324 (1985).

41. R. K. Ellis, Fermilab preprint 86/35-T (1986).

42. From V. Barger and R. J. N. Phillips, **Collider Physics**, Frontiers of Physics (to be published).

43. E. W. N. Glover, F. Halzen, and A. D. Martin, Phys. Lett. **176B**, 480 (1986).

Table 1a. Input data and experimental errors.

quantity	mean value	error
$\mid U_{ud} \mid$	0.9744	0.001
$\mid U_{us} \mid$	0.220	0.002
$\mid U_{cd} \mid$	0.207	0.024
$\mid U_{cs} \mid$	0.95	0.14
$\frac{\mid U_{ub} \mid}{\mid U_{cb} \mid}$	≤ 0.20	-
B_{sl}	0.11	0.01
τ_B (10^{-12}s)	1.16	0.14
m_B (GeV)	5.2752	0.0028
m_W (GeV)	81.8	1.5
ϵ (10^{-3})	2.275	0.021
$\frac{\Delta M}{\Gamma}$	0.73	0.18

Table 1b. Parameters of the problem and their range of variation.

parameter	minimum value	maximum value
s_1	0.21	0.23
s_2	0.	0.15
s_3	0.	0.1
δ	0.	2π
$\Lambda_{\rm QCD}$	0.1	0.4
m_c	1.1	1.8
m_b	4.6	5.2
m_t	20	100
B_K	0.3	1
$f_B^2 \times B_B$	0.01	$0.1 - \begin{cases} 0.06 \\ 0.04 \\ 0.03 \end{cases}$

FIGURE CAPTIONS

Fig. 1. Progress in jet cross section measurements in $p\bar{p}$ collisions.

Fig. 2a. Almost universal angular distribution of $2 \to 2$ parton cross sections.

Fig. 2b. Comparison with data on $gg \to gg$ (from $p\bar{p}$ colliders) and $e^+e^- \to e^+e^-$ (from e^+e^- colliders).

Fig. 3. $O(\alpha\alpha_s)$ and $O(\alpha\alpha_s^2)$ diagrams for direct photon production.

Fig. 4. Direct photon cross section compared with the leading order prediction (dashed line) and with a calculation including the next-to-leading-order contributions.

Fig. 5. Radiation zero in the angular distribution of the photon relative to the beams for the process $u\bar{d} \to u\bar{d}\gamma$. The zero is absent with Han-Nambu quark charge assignments. For a detailed discussion of the calculations, see Ref. 10.

Fig. 6. Amplitude and squared amplitude of the process $qq \to qq\gamma$.

Fig. 7a,b. Sample calculations of inclusive jet cross sections.

Fig. 8. Inclusive minijet cross section measured by UA1 is fitted to Eq. (1.6) with $p_{T\min} = 3$ GeV and $d\sigma/dp_T$ from Fig. 1. The rise with energy of the total cross section is shown for comparison.

Fig. 9. Radiative corrections to the weak decay $\mu^- \to e^-\bar{\nu}_e\nu_\mu$ involve diagrams with t-quark and Higgs boson (ϕ) intermediate states.

Fig. 10. Relation[17] between M_W and M_Z before (dashed) and after (solid line) radiative corrections. The relation is shown for three possible values of M_Z and for a range of values of the t-quark mass.

Fig. 11. Relation between M_W/M_Z and m_t from Fig. 2 for M_Z=91.5 GeV (solid line). The errors reflect the measurement errors on M_Z. The dashed line is the UA2 result for M_W/M_Z and is compatible with the predicted value for $m_t \lesssim 300$ GeV.

Fig. 12. Higher order diagrams contribution to the inequality of $q\bar{q} \to W$ and $q\bar{q} \to Z$ cross sections.

Fig. 13. The ratio of W, Z production cross sections in $p\bar{p}$ interactions is calculated by extracting the difference between u, d parton flux factors from a series of experiments. We assumed that $M_W = 80.1$ GeV and fixed M_Z from $\sin^2\theta_W = 0.232$. After including the errors on these quantities we obtain $\sigma_W/\sigma_Z = 3.42 \pm 0.05$.

Fig. 14. Dependence of R on the top mass assuming 3 generations of quarks and leptons. The calculation is compared with the measured value obtained by combining UA1 and UA2 results.

Fig. 15. Probability that the calculation and measured values of R in Fig. 6 are compatible.

Fig. 16. R is reduced from its standard model value (SM) by mixing Z with a heavy Z'. The mixing angle has been maximized within allowed limits on the mass and couplings of a heavy Z'.

Fig. 17. Equality of $W(\to e\nu)$ (dashed line) and $Z(\to \nu\bar{\nu})$ events (full line) at large p_T for $N_\nu = 3$. The theoretical calculation is compared to UA2 data on $W \to e\nu$ and UA1 data represented by the histograms. The dashed (solid) histogram represets the $Z \to \nu\nu$ ($W \to e\nu$) rates. Although the equality is satisfied, there is a possible excess compared to the theoretical calculation. This excess is associated with possible anomalous 2-jet events.

Fig. 18. The mass difference and ϵ-parameter of the neutral K system provide information on charm and top masses via the diagrams shown. Similarly mixing of B and $\bar{B}$ is sensitive to m_t.

Fig. 19. Probability that a value of m_t is compatible with all information listed in Table 1a. This includes $\Delta M/\Gamma$ of the B-$\bar{B}$ system.

Fig. 20. Eurojet calculation of single and dilepton cross section from c, b decay. Also shown is the additional prompt lepton yield from a top with mass $23 \sim 40$ GeV. Data from UA1.

Fig. 21a. Representative diagrams for the production of heavy quarks.

Fig. 21b. Production of a heavy quark associated with a high p_T jet.

Fig. 22. Bethe-Heitler (α^3) dominates Compton scattering (α^2) when high energy photons interact with matter.

Fig. 23. Mass singularity (almost real exchange gluon) of the $2 \rightarrow 3$ diagram is included in the $2 \rightarrow 2\,gg \rightarrow Q\bar{Q}$ diagram via the evolution of the gluon structure function.

Fig. 24. Heavy quark production cross sections in $p\bar{p}$ interactions as a function of energy. Arrows indicate present and future ACOL sensitivity.

Fig. 25a,b. Invariant mass of dileptons (a) $\mu^+\mu^-$, (b) e^+e^-, from semi-leptonic decay of c, b, t (40 GeV) pairs in $p\bar{p}$ interaction ($\sqrt{s} = 540$ GeV). Cuts on the p_T of the leptons and Drell-Yan backgrounds are also shown.

Fig. 25c. Invariant mass of dileptons $e\mu$ from semi-leptonic decay of c, b, t (40 GeV) pairs in $p\bar{p}$ interaction ($\sqrt{s} = 540$ GeV). Cuts on the p_T of the leptons are the same as in (a) and (b).

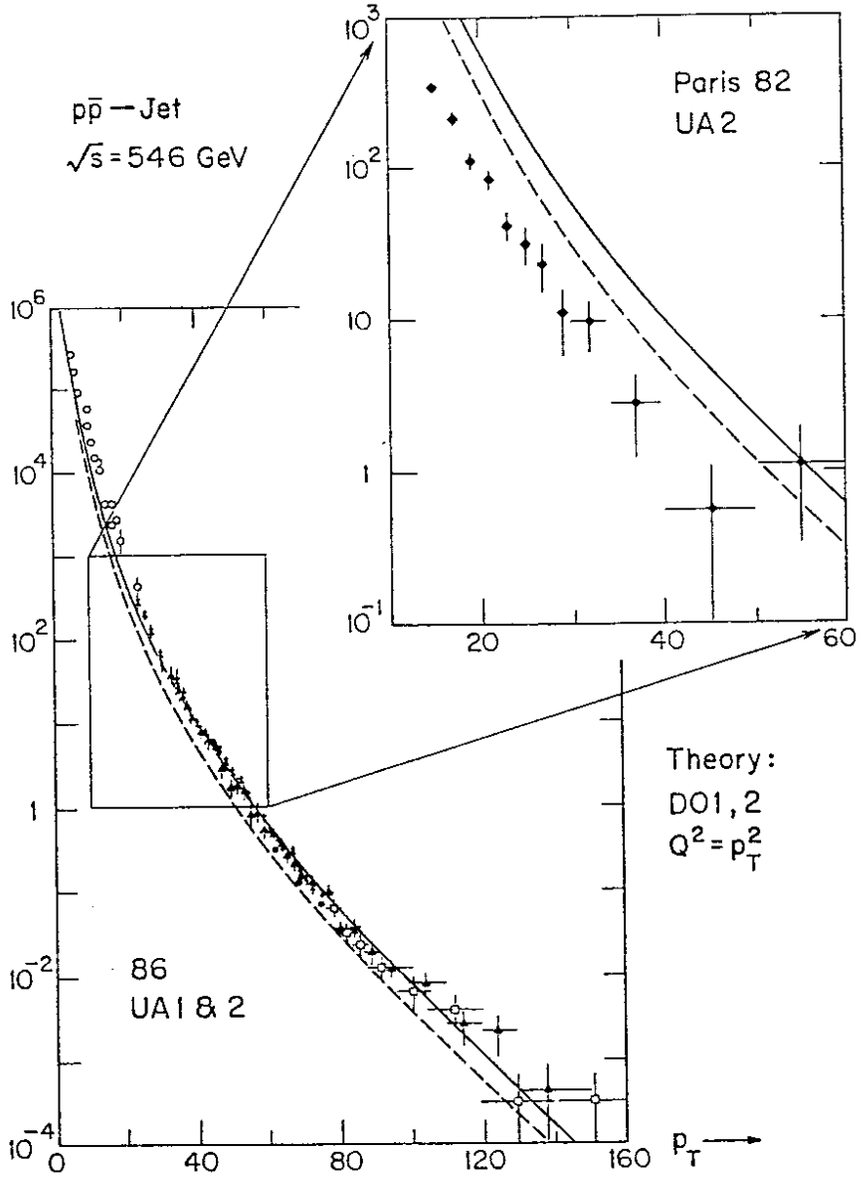
pp̄ → Jet
√s = 546 GeV
Paris 82
UA2
Theory:
DO1, 2
Q² = p_T²
86
UA1 & 2
p_T

Fig. 1

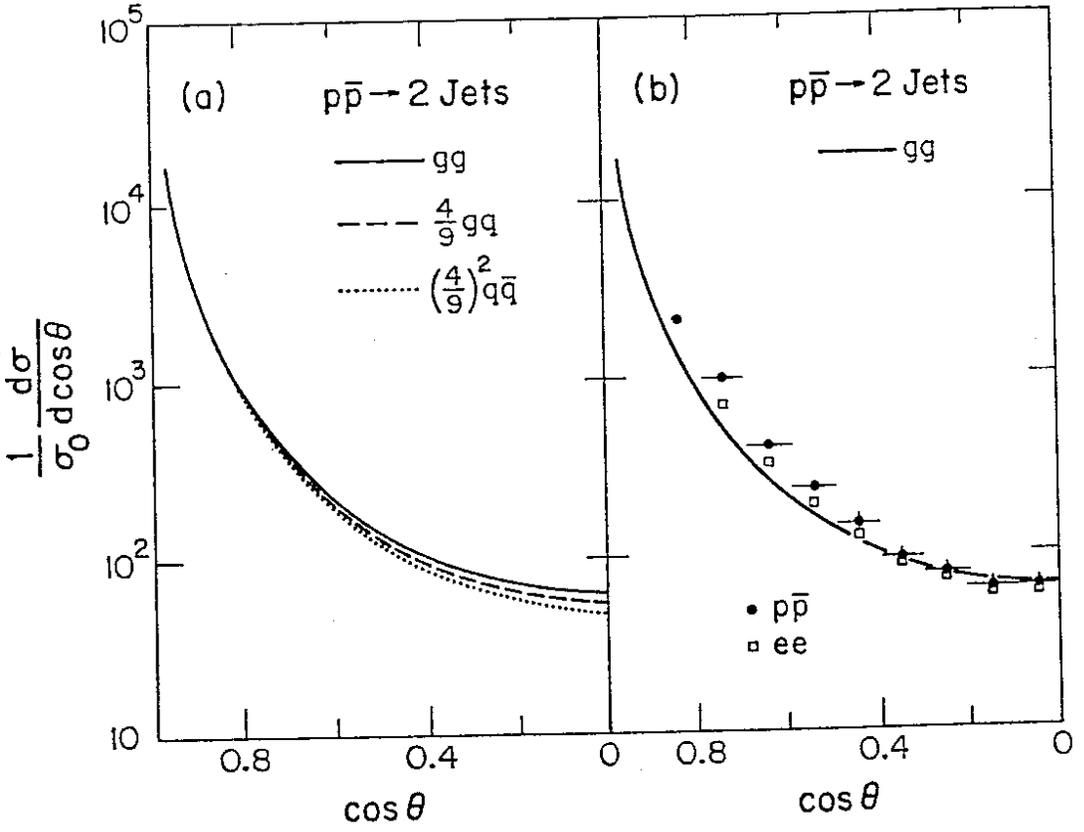
(a)
pp̄ → 2 Jets
gg
4/9 gq
(4/9)² qq̄
(b)
pp̄ → 2 Jets
gg
pp̄
ee
1/σ₀ dσ/dcosθ
cos θ
cos θ

Fig. 2

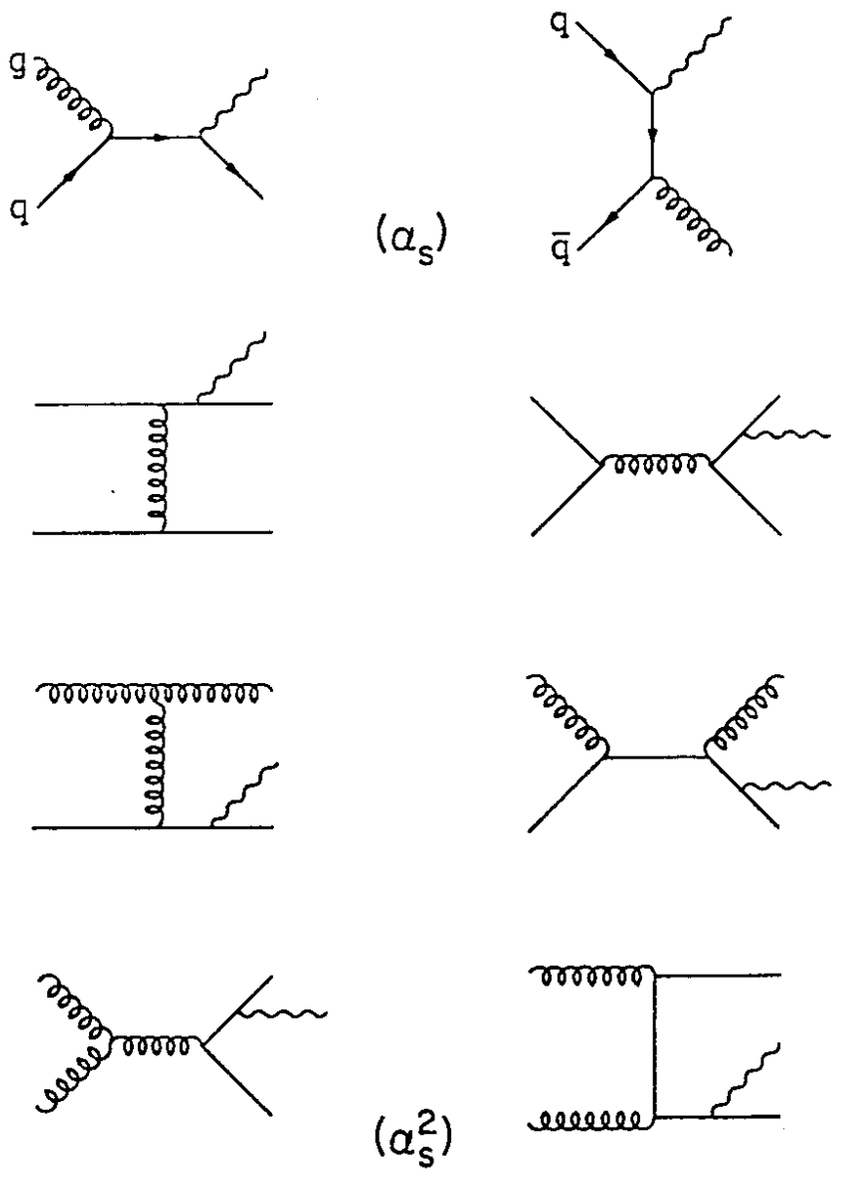
g
q
q
(α_s)
q
$\bar{q}$
(α_s^2)

Fig. 3

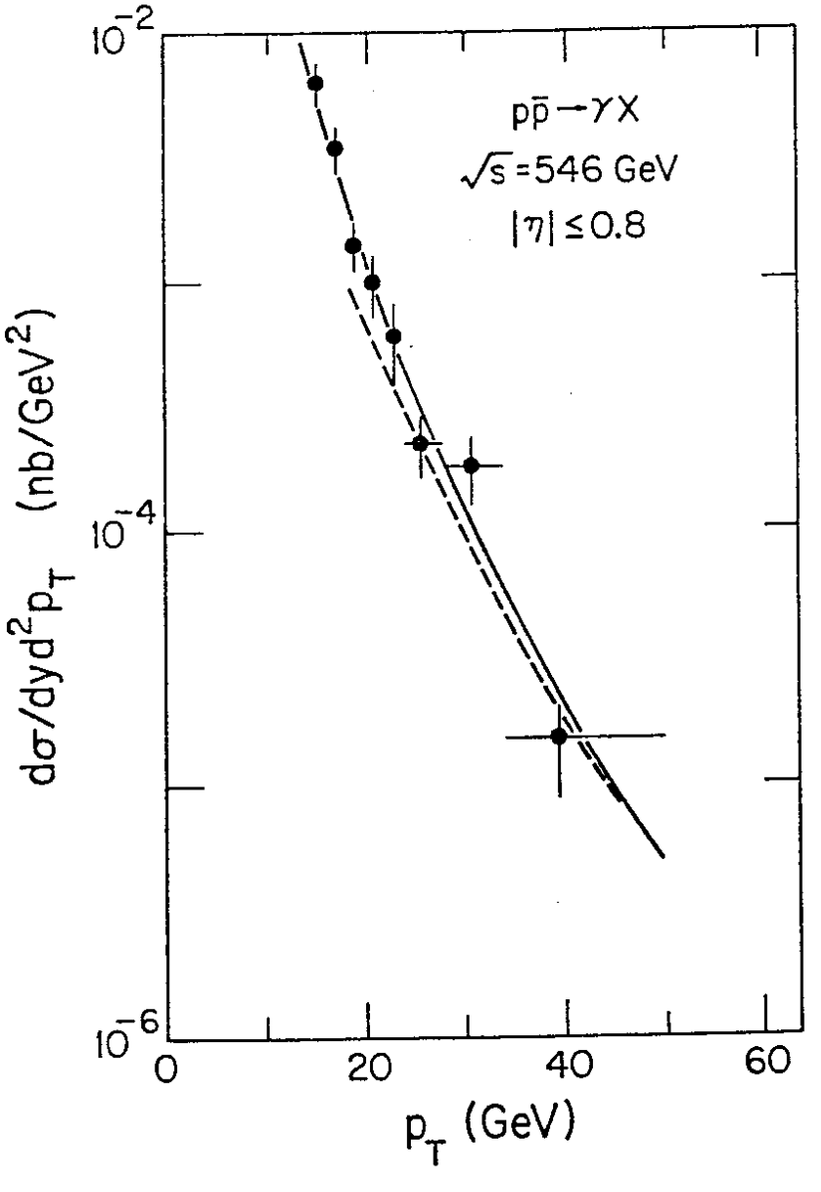
$p\bar{p} \rightarrow \gamma X$
$\sqrt{s} = 546$ GeV
$|\eta| \leq 0.8$
$d\sigma/dy d^2p_T$ (nb/GeV^2)
10^{-2}
10^{-4}
10^{-6}
0
20
40
60
p_T (GeV)

Fig. 4

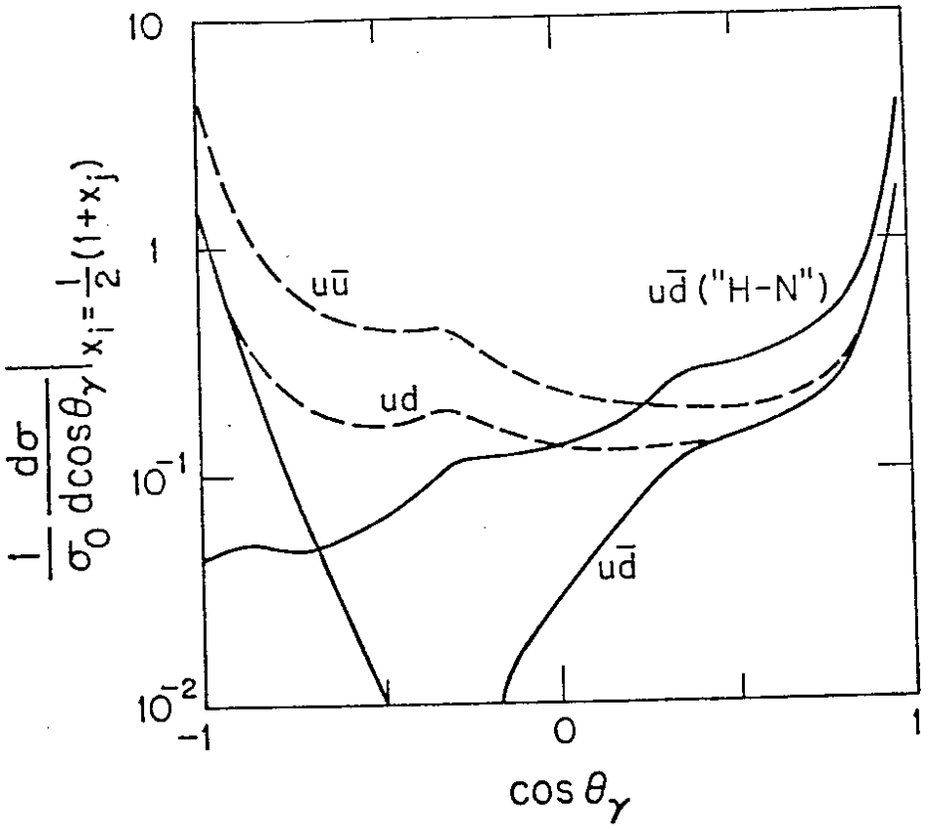
10
1
10^{-1}
10^{-2}
-1
0
1
$\cos\theta_\gamma$
$\frac{1}{\sigma_0}\frac{d\sigma}{d\cos\theta_\gamma}\Big|_{x_i=\frac{1}{2}(1+x_j)}$
$u\bar{u}$
$u\bar{d}$ ("H-N")
ud
$u\bar{d}$

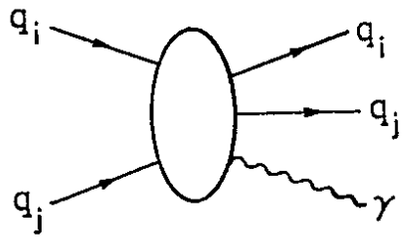
q_i
q_j
q_i
q_j
γ

Fig. 5

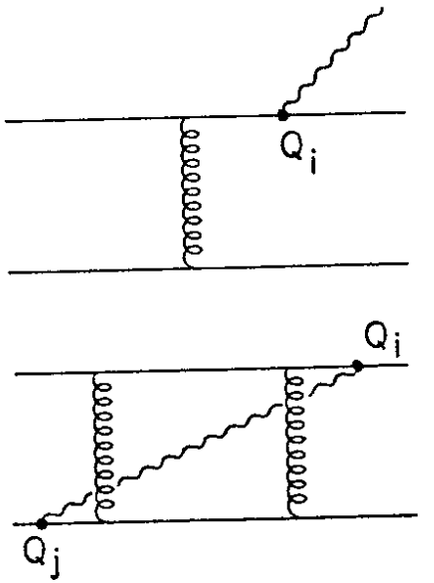
Q_i
Q_i
Q_j

Fig. 6

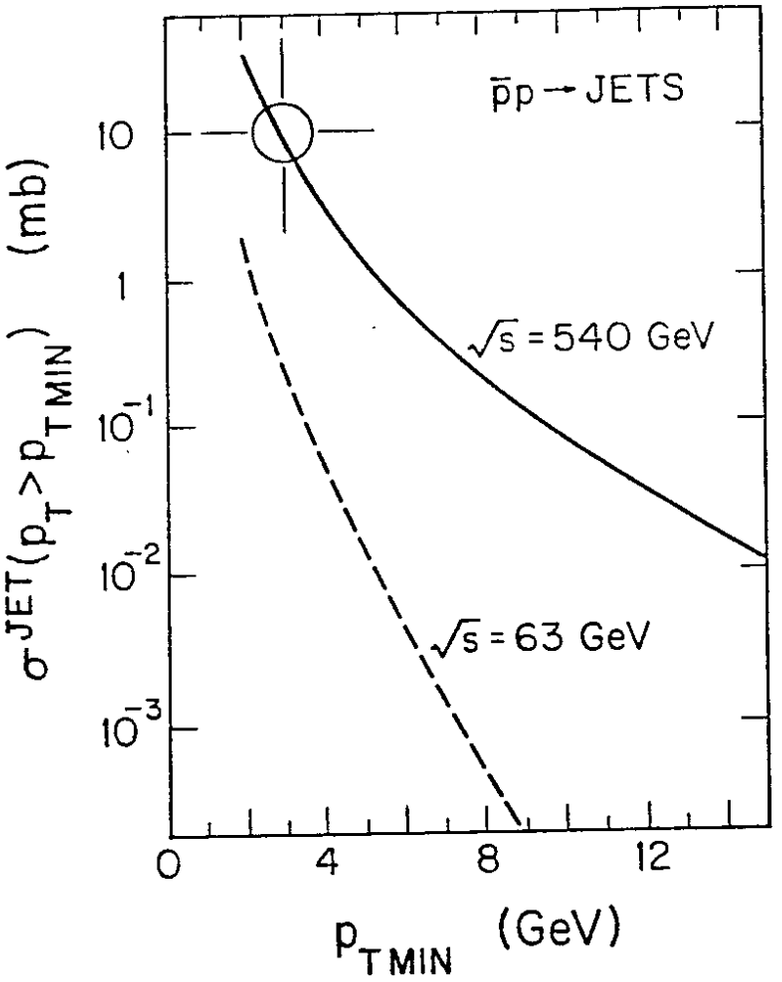
$\bar{p}p \rightarrow$ JETS
$\sqrt{s}$ = 540 GeV
$\sqrt{s}$ = 63 GeV
$\sigma^{JET}(p_T > p_{T\,MIN})$ (mb)
$p_{T\,MIN}$ (GeV)
10
1
10^{-1}
10^{-2}
10^{-3}
0
4
8
12

Fig. 7(a)

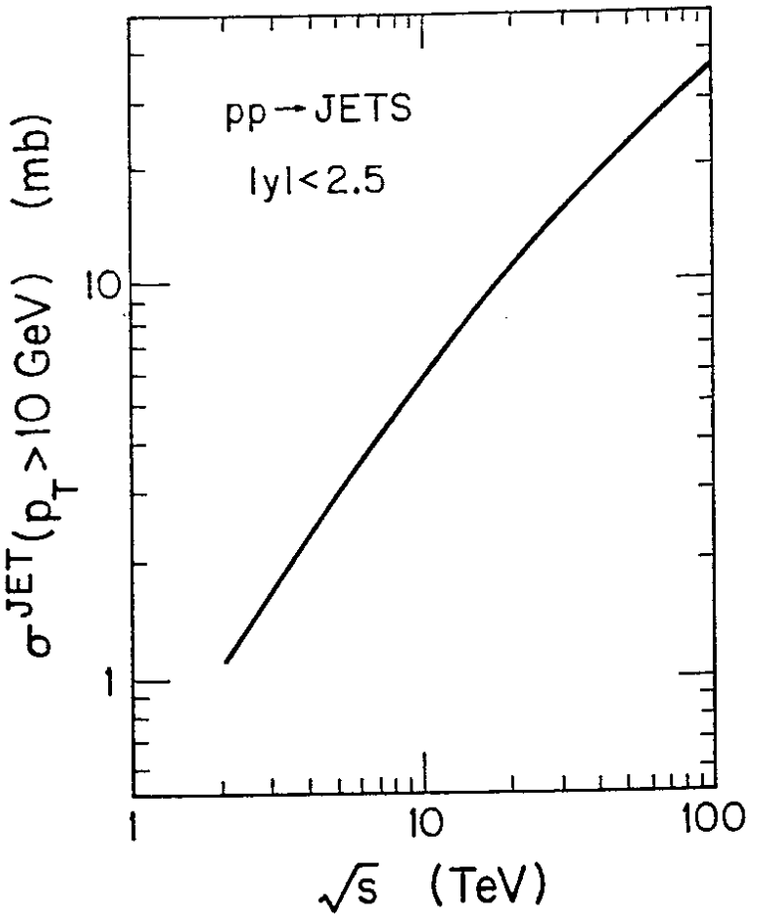
$pp \rightarrow$ JETS
$|y| < 2.5$
$\sigma^{JET}(p_T > 10\,GeV)$ (mb)
$\sqrt{s}$ (TeV)
10
1
1
10
100

Fig. 7(b)

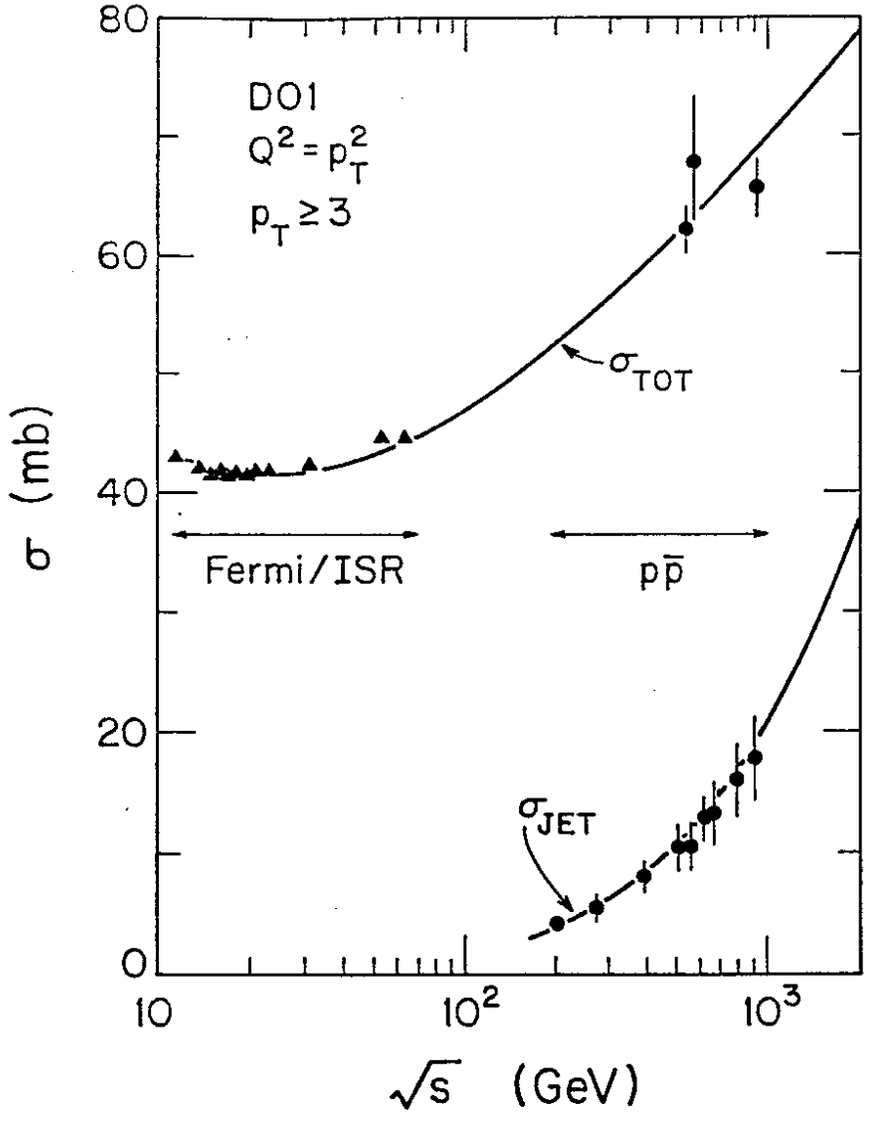
80
60
40
20
0
σ (mb)
DO1
$Q^2 = p_T^2$
$p_T \geq 3$
σ_{TOT}
Fermi/ISR
$p\bar{p}$
σ_{JET}
10
10^2
10^3
$\sqrt{s}$ (GeV)

Fig. 8

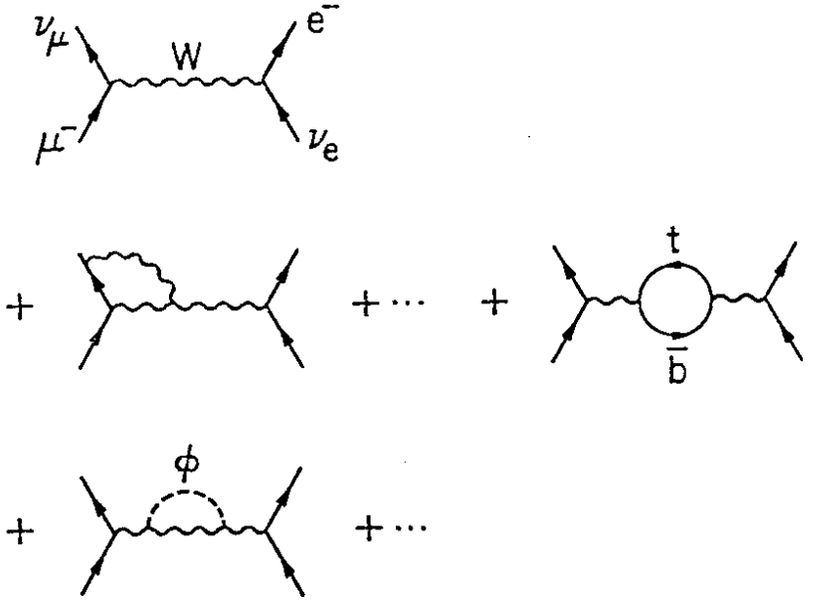
ν_μ
μ^-
W
e^-
ν_e
+
+ ⋯
+
t
$\bar{b}$
+
ϕ
+ ⋯

Fig. 9

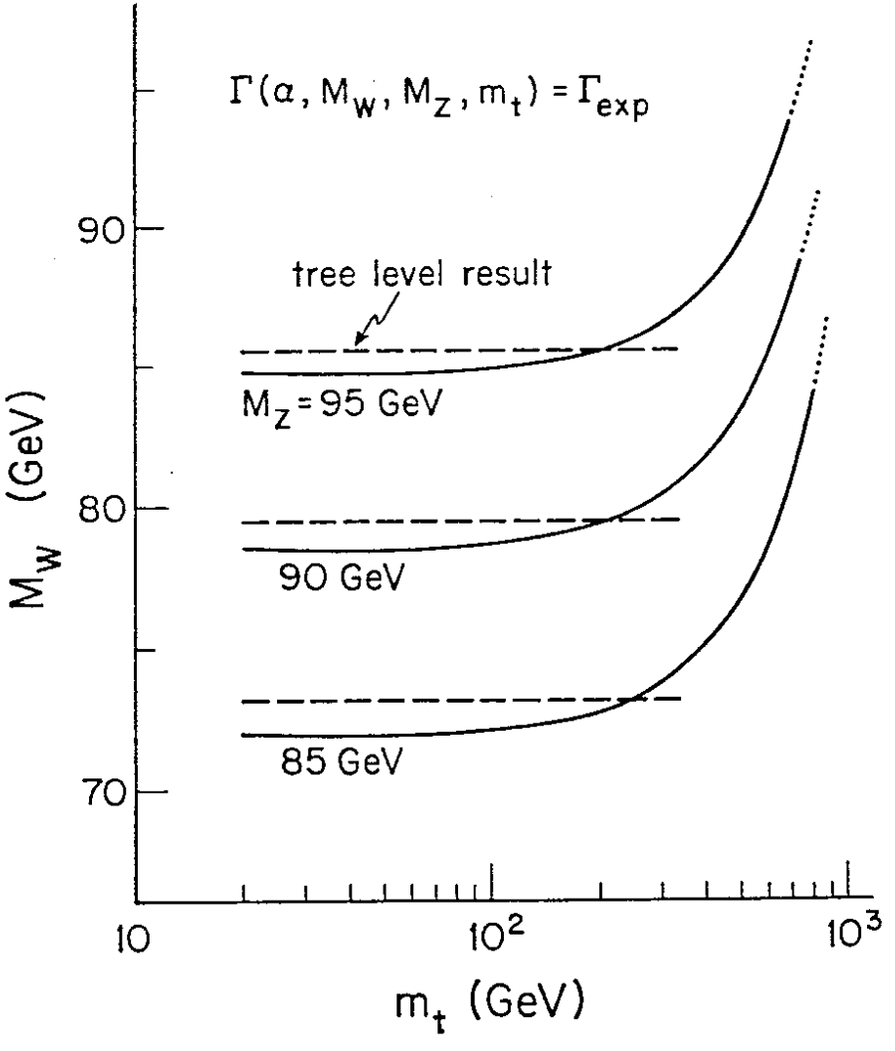
$\Gamma(\alpha, M_W, M_Z, m_t) = \Gamma_{exp}$
tree level result
$M_Z = 95$ GeV
90 GeV
85 GeV
90
80
70
M_W (GeV)
10
10^2
10^3
m_t (GeV)

Fig. 10

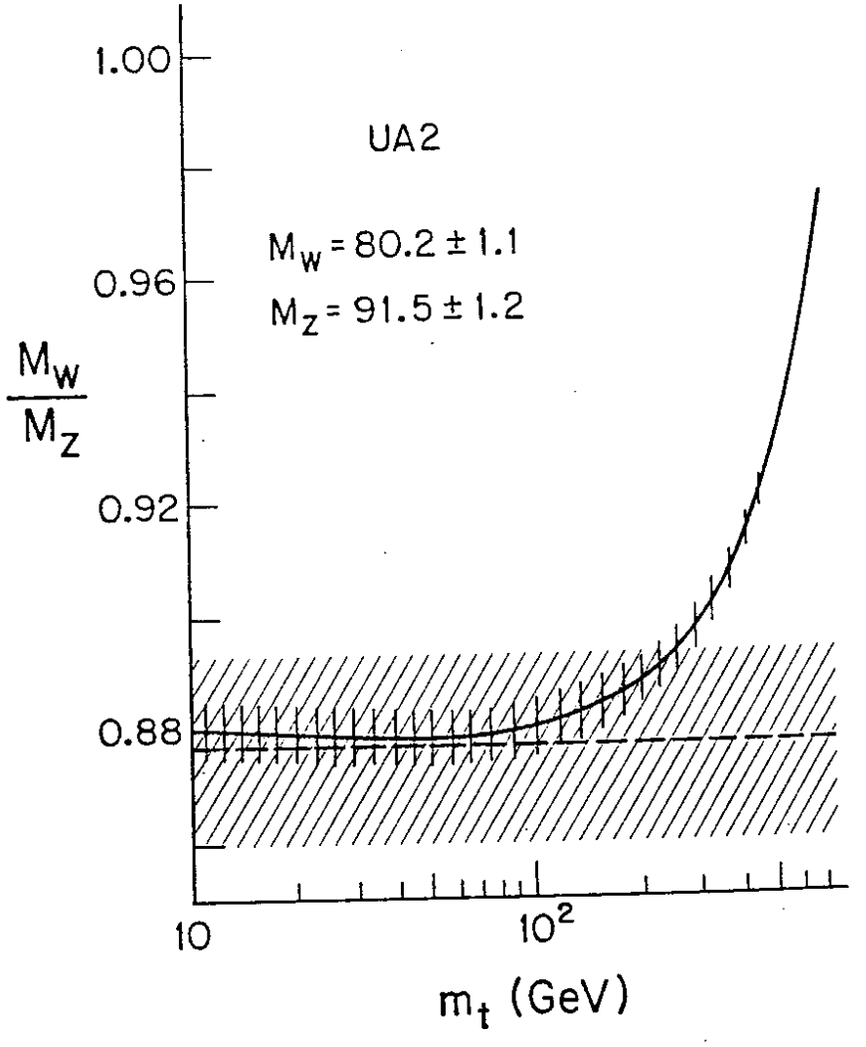
UA2
$M_W = 80.2 \pm 1.1$
$M_Z = 91.5 \pm 1.2$
1.00
0.96
0.92
0.88
$\frac{M_W}{M_Z}$
10
10^2
m_t (GeV)

Fig. 11

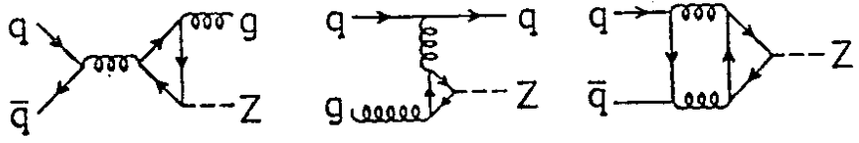
q
q̄
g
Z
q
q
g
Z
q
q̄
Z

Fig. 12

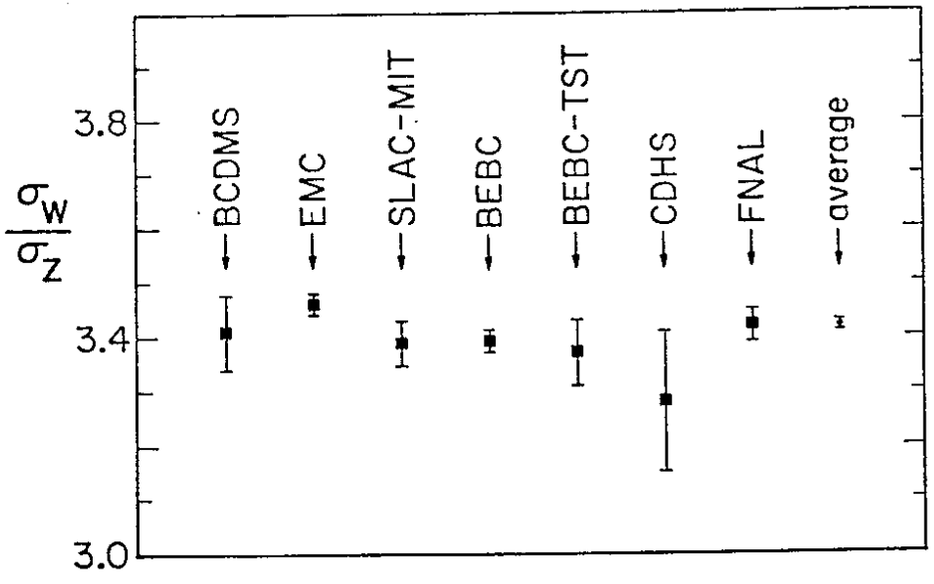
3.8
3.4
3.0
$\frac{g_W}{g_Z}$
BCDMS
EMC
SLAC-MIT
BEBC
BEBC-TST
CDHS
FNAL
average

Fig. 13

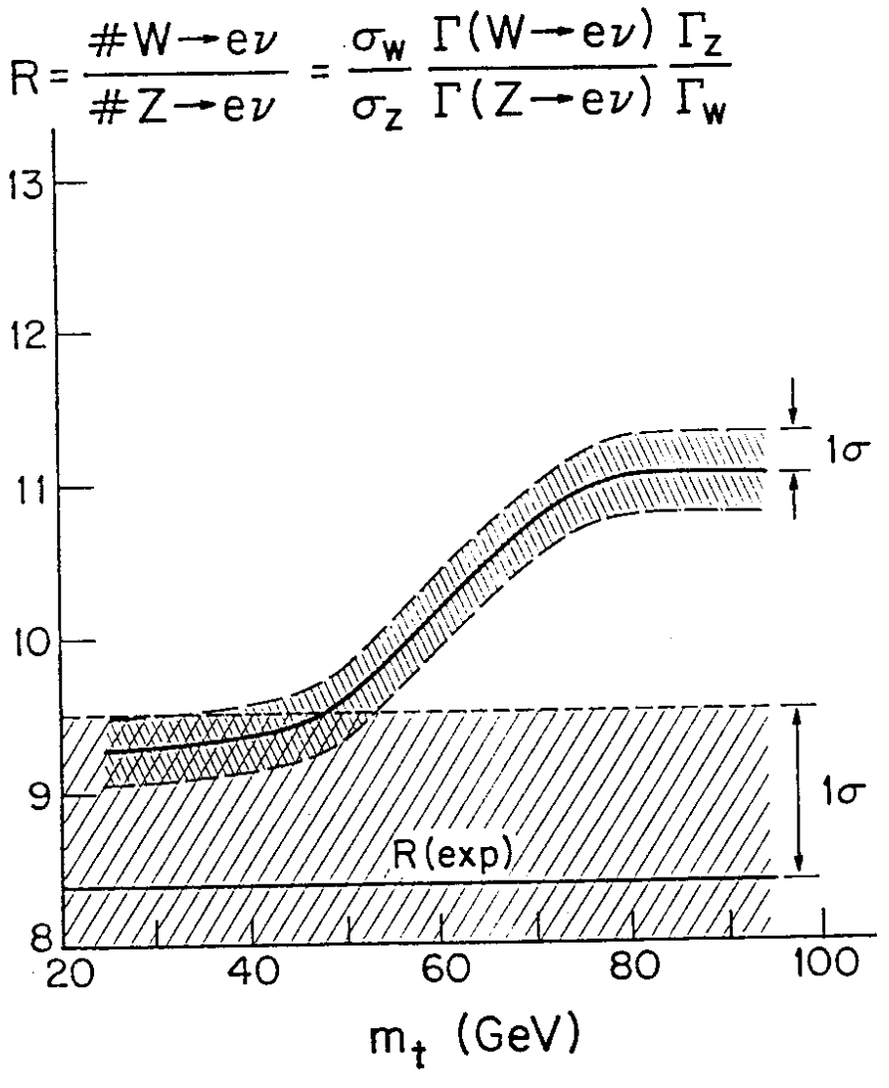
R = #W→eν / #Z→eν = σW/σZ Γ(W→eν)/Γ(Z→eν) ΓZ/ΓW
13
12
11
10
9
8
1σ
1σ
R(exp)
20
40
60
80
100
mt (GeV)

Fig. 14

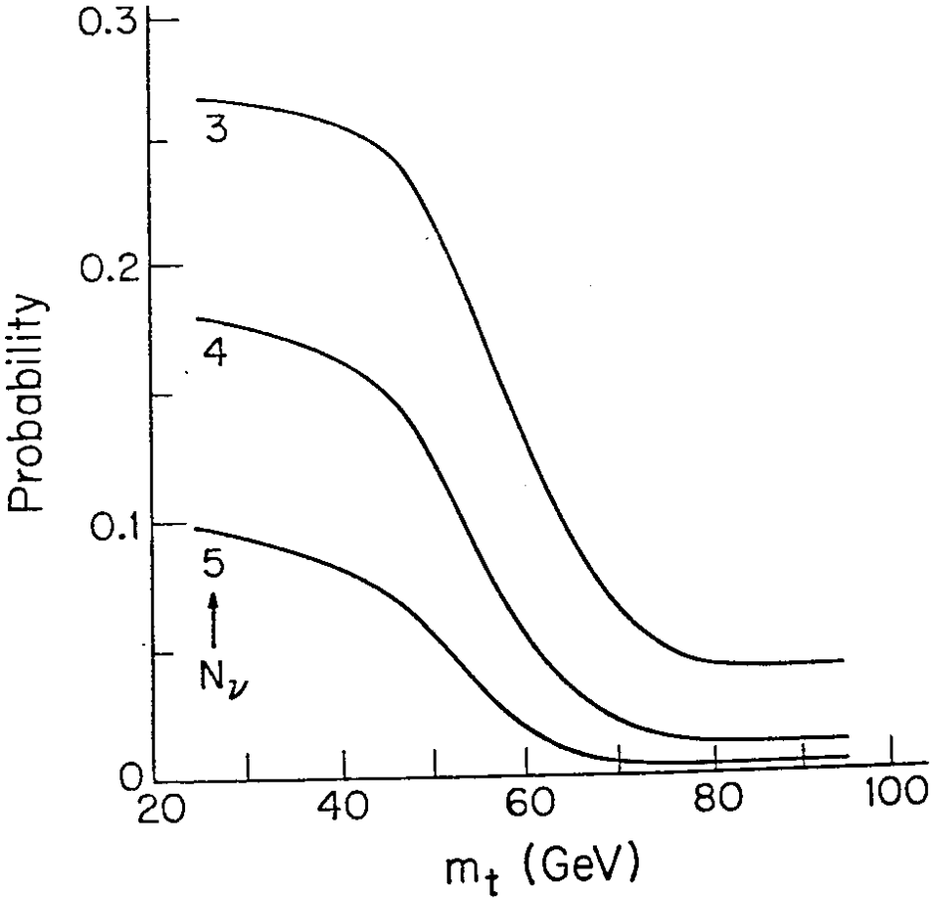
0.3
0.2
0.1
0
Probability
3
4
5
Nν
20
40
60
80
100
mt (GeV)

Fig. 15

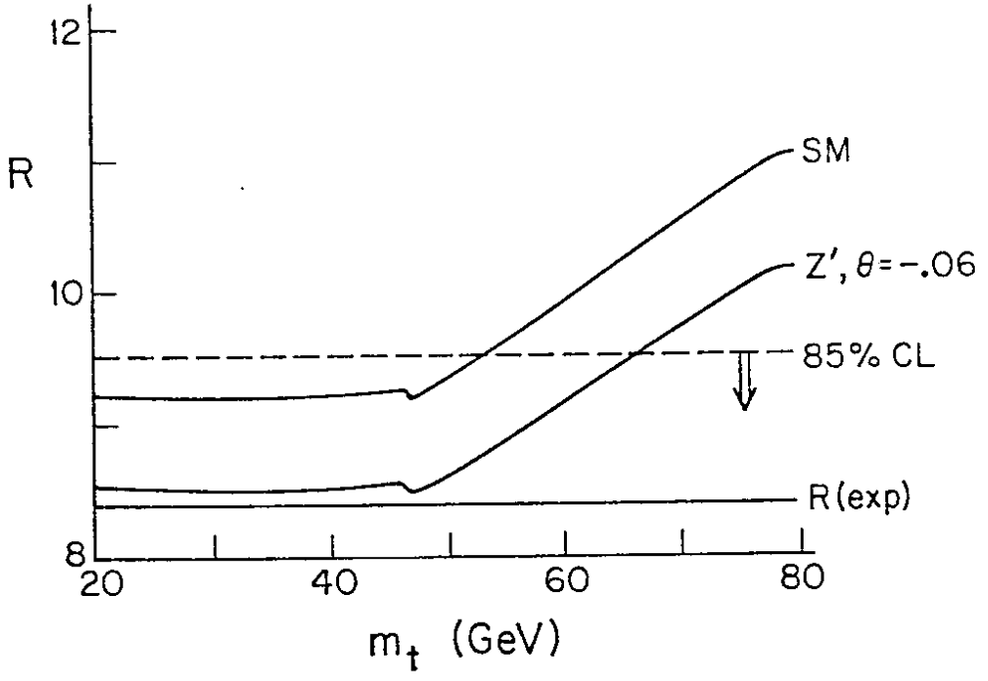
12
10
8
R
SM
Z', θ=-.06
85% CL
R(exp)
20
40
60
80
m_t (GeV)

Fig. 16

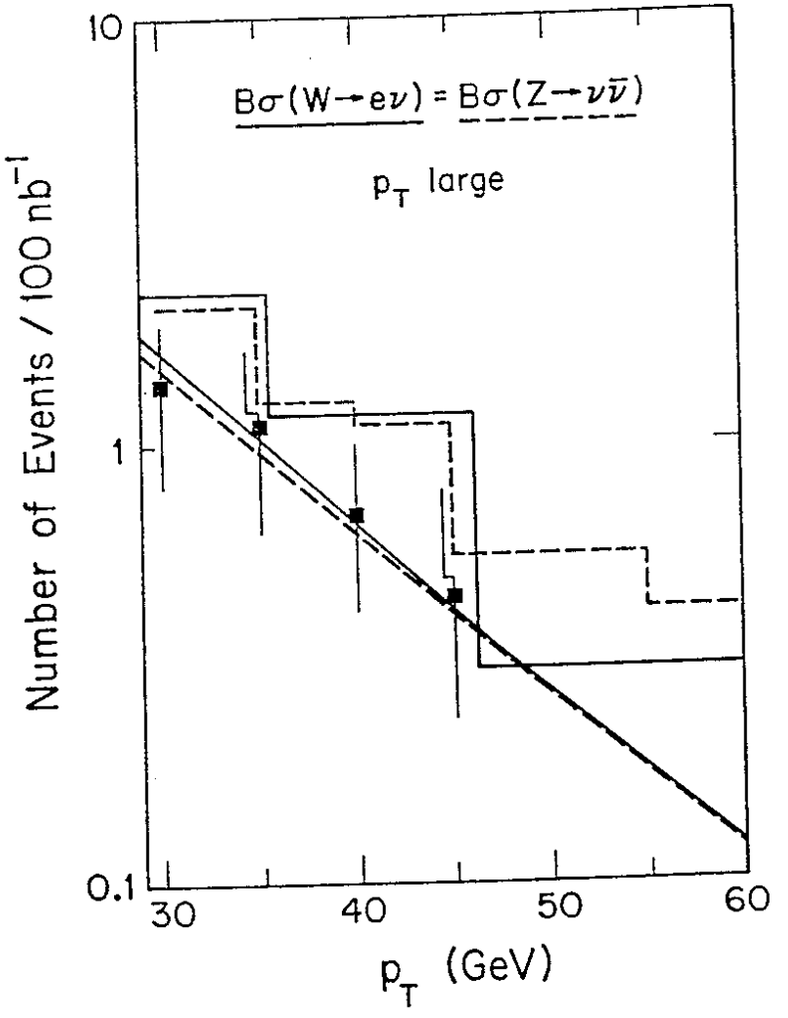
10
1
0.1
Bσ(W→eν) = Bσ(Z→νν̄)
p_T large
Number of Events / 100 nb^-1
30
40
50
60
p_T (GeV)

Fig. 17

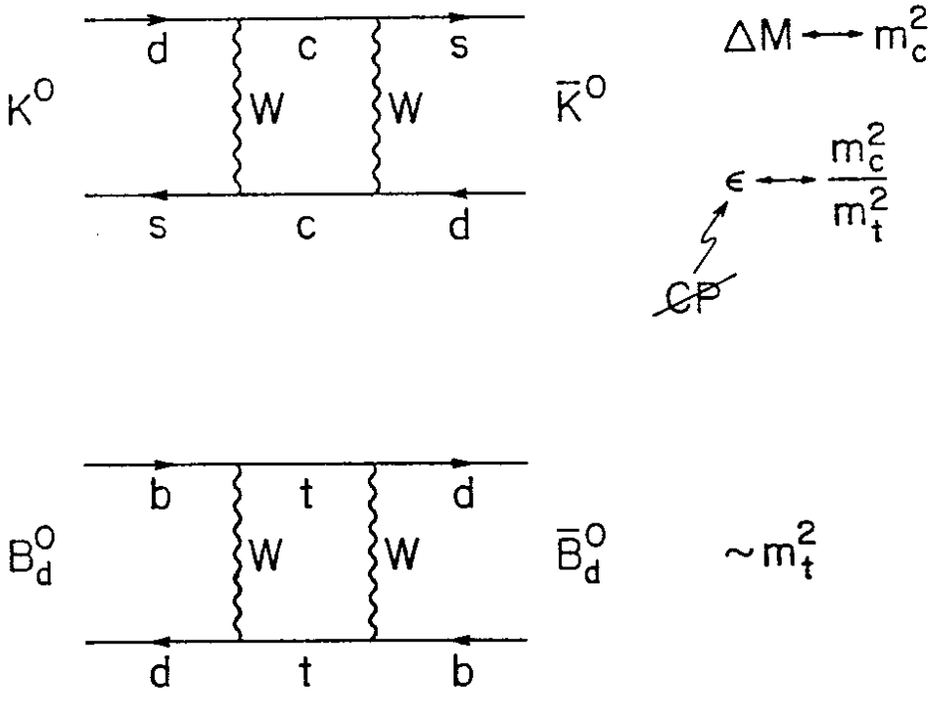
d
c
s
W
W
K^0
$\bar{K}^0$
s
c
d
$\Delta M \longleftrightarrow m_c^2$
$\epsilon \longleftrightarrow \frac{m_c^2}{m_t^2}$
CP
b
t
d
W
W
B_d^0
$\bar{B}_d^0$
d
t
b
$\sim m_t^2$

Fig. 18

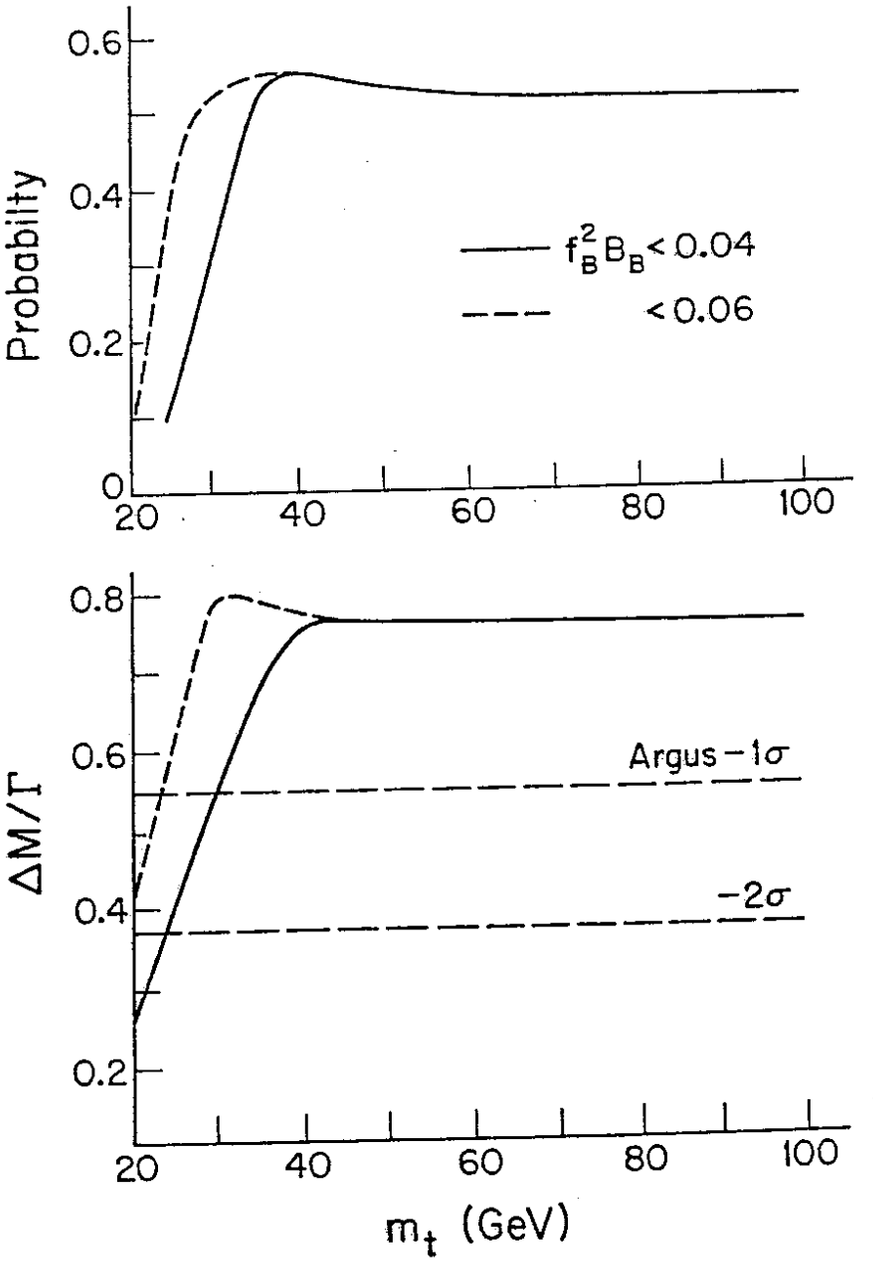
Probability
0.6
0.4
0.2
0
20
40
60
80
100
$f_B^2 B_B < 0.04$
< 0.06
$\Delta M/\Gamma$
0.8
0.6
0.4
0.2
Argus -1σ
-2σ
m_t (GeV)

Fig. 19

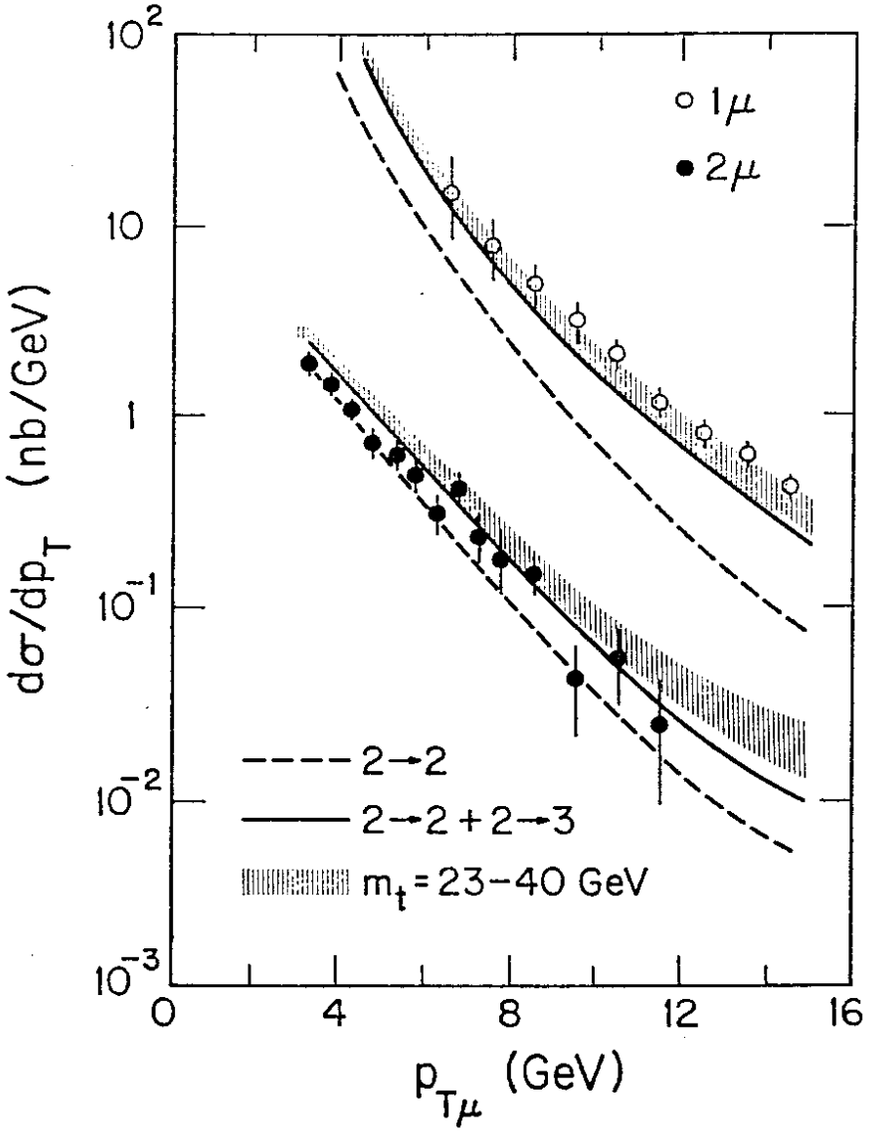

Fig. 20

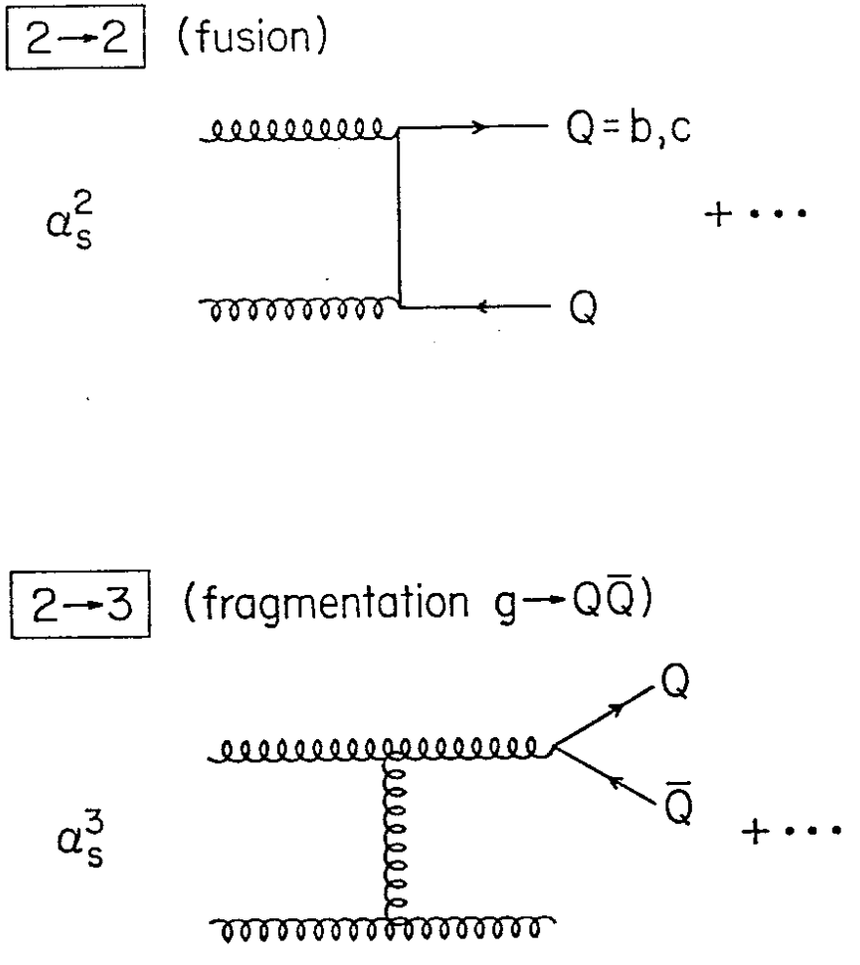

Fig. 21(a)

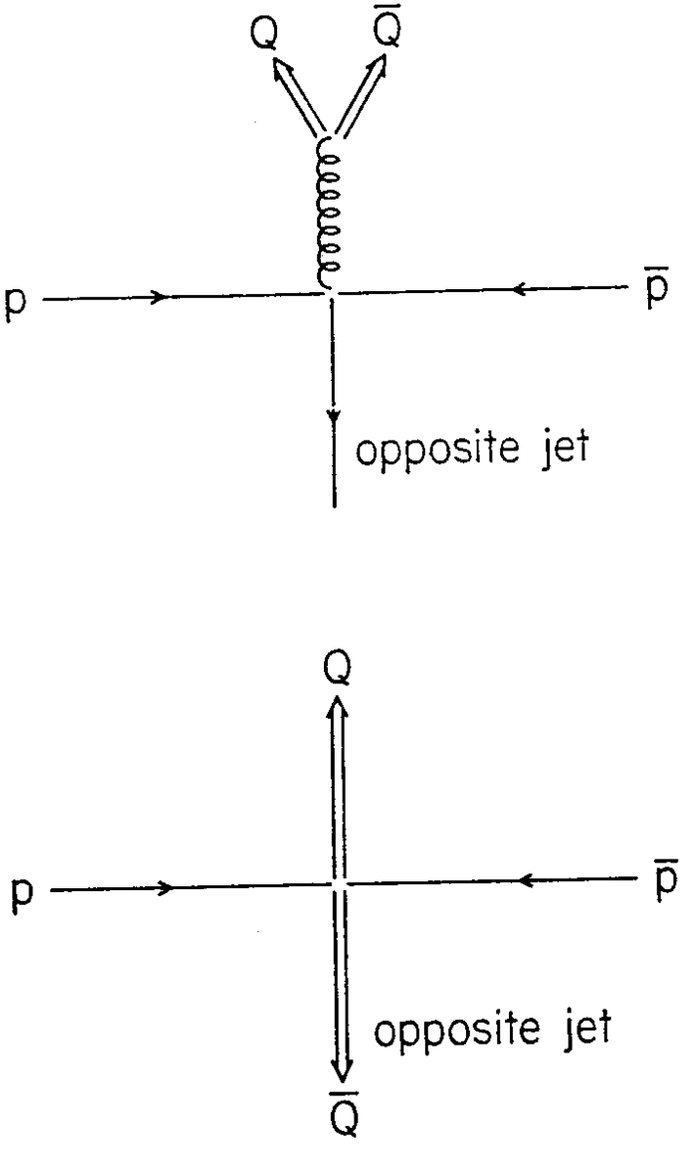

Fig. 21(b)

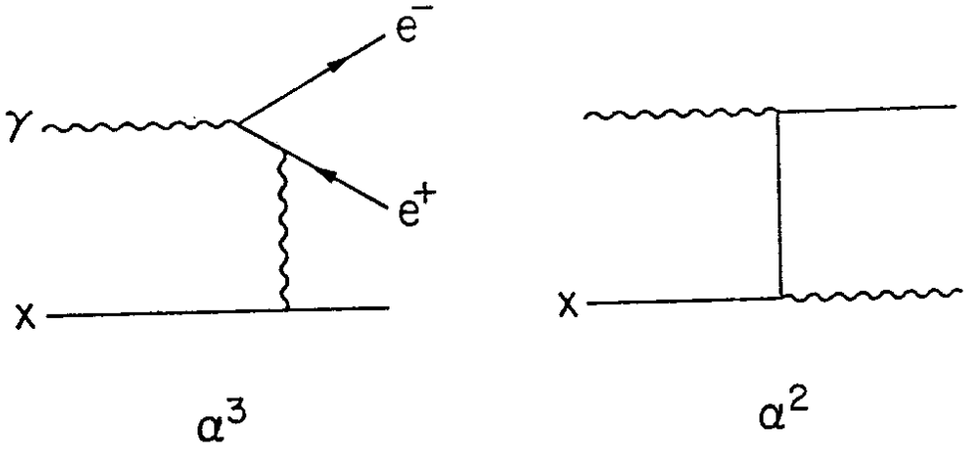

Fig. 22

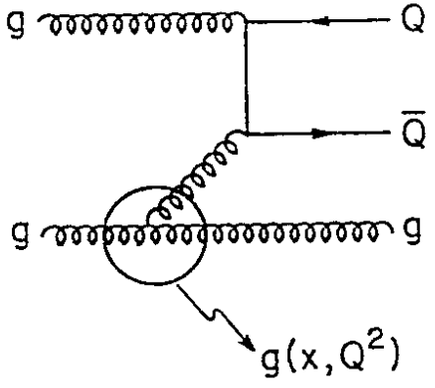
g
Q
$\bar{Q}$
g
g
$g(x,Q^2)$

Fig. 23

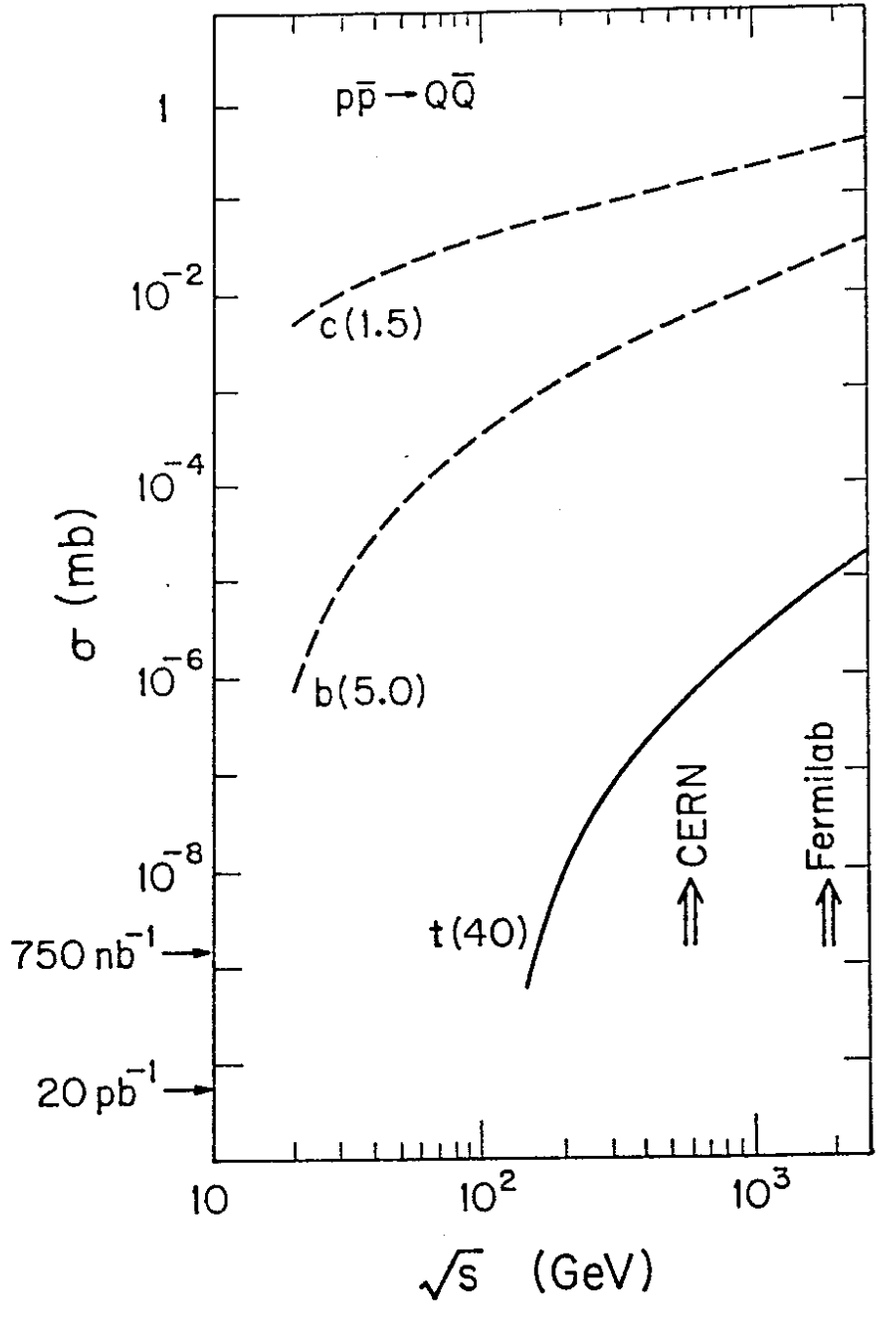
$p\bar{p} \to Q\bar{Q}$
1
10^{-2}
10^{-4}
10^{-6}
10^{-8}
σ (mb)
c(1.5)
b(5.0)
t(40)
750 nb^{-1}
20 pb^{-1}
CERN
Fermilab
10
10^2
10^3
$\sqrt{s}$ (GeV)

Fig. 24

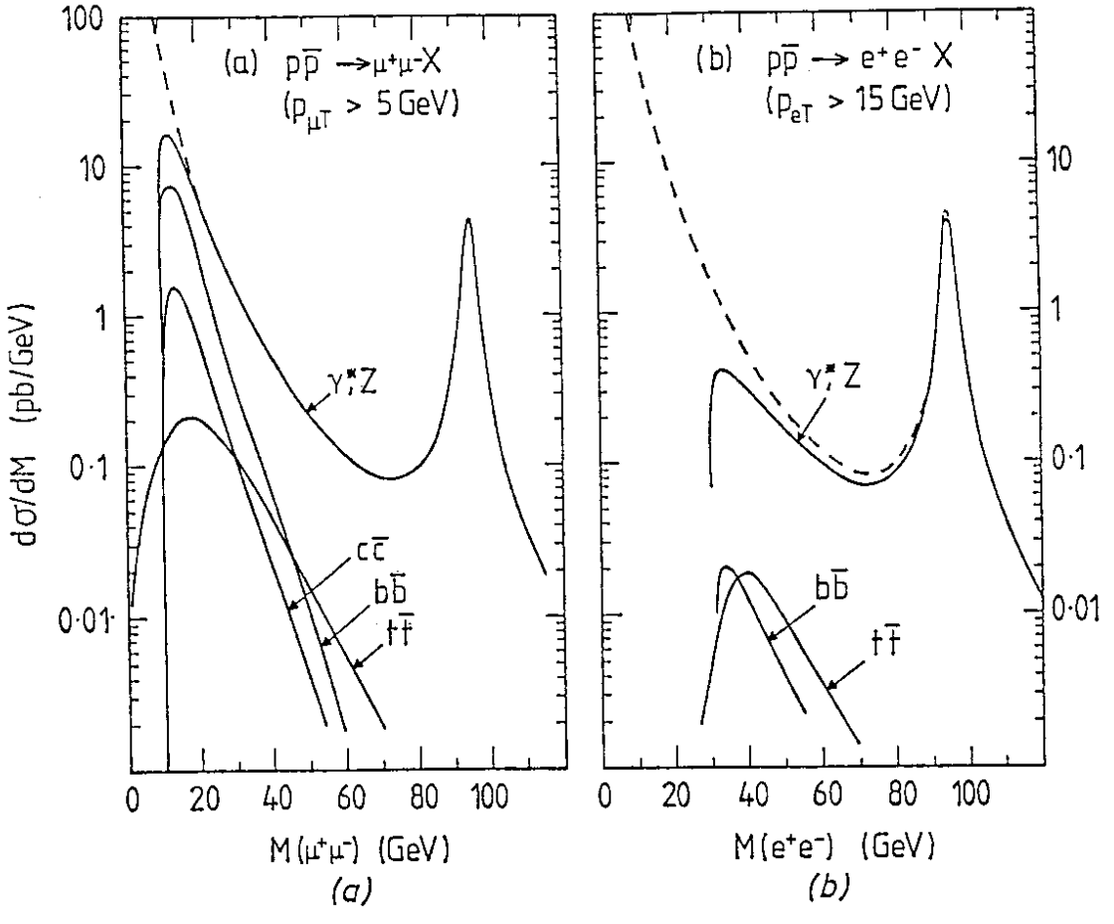

Figs. 25(a), (b)

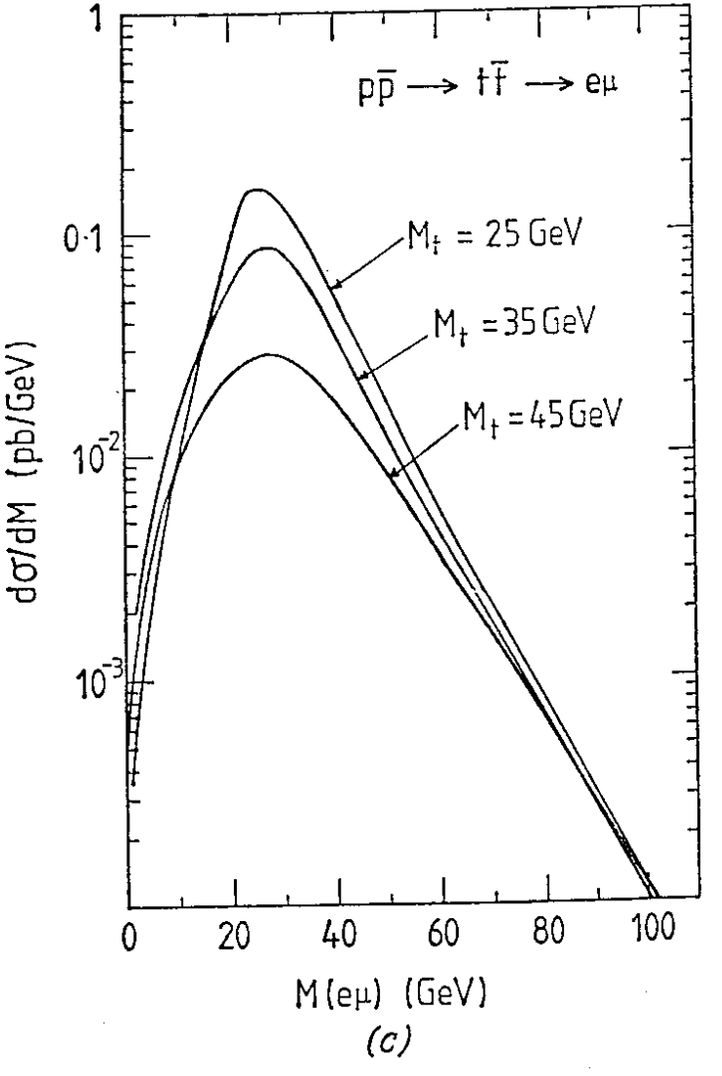

Fig. 25(c)